PARAMETER ESTIMATION OF DYNAMIC AIR-CONDITIONING COMPONENT MODELS USING LIMITED SENSOR DATA

A Thesis

by

NATARAJKUMAR HARIHARAN

Submitted to the Office of Graduate Studies of
Texas A&M University
in partial fulfillment of the requirements for the degree of

MASTER OF SCIENCE

May 2010

Major Subject: Mechanical Engineering

PARAMETER ESTIMATION OF DYNAMIC AIR-CONDITIONING COMPONENT MODELS USING LIMITED SENSOR DATA

A Thesis

by

NATARAJKUMAR HARIHARAN

Submitted to the Office of Graduate Studies of
Texas A&M University
in partial fulfillment of the requirements for the degree of

MASTER OF SCIENCE

Approved by:

Chair of Committee,	Bryan Rasmussen
Committee Members,	Jorge Alvarado
	Alan Palazzolo
Head of Department,	Dennis O'Neal

May 2010

Major Subject: Mechanical Engineering

ABSTRACT

Parameter Estimation of Dynamic Air-conditioning Component Models Using Limited Sensor Data. (May 2010)

Natarajkumar Hariharan, B.E., Birla Institute of Technology, Ranchi

Chair of Advisory Committee: Dr. Bryan Rasmussen

This thesis presents an approach for identifying critical model parameters in dynamic air-conditioning systems using limited sensor information. The expansion valve model and the compressor model parameters play a crucial role in the system model's accuracy. In the past, these parameters have been estimated using a mass flow meter; however, this is an expensive devise and at times, impractical. In response to these constraints, a novel method to estimate the unknown parameters of the expansion valve model and the compressor model is developed. A gray box model obtained by augmenting the expansion valve model, the evaporator model, and the compressor model is used. Two numerical search algorithms, nonlinear least squares and Simplex search, are used to estimate the parameters of the expansion valve model and the compressor model. This parameter estimation is done by minimizing the error between the model output and the experimental systems output. Results demonstrate that the nonlinear least squares algorithm was more robust for this estimation problem than the Simplex search algorithm.

In this thesis, two types of expansion valves, the Electronic Expansion Valve and the Thermostatic Expansion Valve, are considered. The Electronic Expansion Valve model is a static model due to its dynamics being much faster than the systems dynamics; the Thermostatic expansion valve model, however, is a dynamic one. The parameter estimation algorithm developed is validated on two different experimental systems to confirm the practicality of its approach. Knowing the model parameters accurately can lead to a better model for control and fault detection applications. In addition to parameter estimation, this thesis also provides and validates a simple usable mathematical model for the Thermostatic expansion valve.

DEDICATION

To my parents and friends

ACKNOWLEDGEMENTS

I would like to thank my thesis adviser, Dr. Bryan Rasmussen and committee members, Dr. Palazzolo and Dr. Alvarado, for their continuous guidance and support over the course of this research work. I would also like to thank Dr. Rasmussen for his insight and encouragement, without which this research would not have been possible. I would like to thank Matt Elliott for his help with the experiments. Thanks to all my colleagues at Thermo-Fluids Control Laboratory for sharing laughs and holding enlightening conversations. I am grateful to all my friends who have helped make my stay in College Station a memorable experience. I would like to thank my parents for their constant support and understanding. Finally, I would like to acknowledge the financial contribution of Honeywell.

NOMENCLATURE

A_1	Area of application of bulb pressure
A_2	Area of application of evaporator pressure
A_o	External surface area of the TEV bulb
A_{rb}	Area of heat conduction between the refrigerant and the bulb
A_v	Area of opening for refrigerant flow in expansion valve
C_b	Specific heat of the TEV bulb
C_d	Coefficient of discharge of the expansion valve
EEV	Electronic Expansion Valve
$HVAC$	Heating, Venting and Air Conditioning
h_o	Heat transfer coefficient between the bulb and the environment
h_{rb}	Heat transfer coefficient between the refrigerant and the bulb
K_s	Spring constant
k_1, k_2	Compressor parameters
$\dot{m}_{air}$	Mass flow rate of the air/secondary coolant over the evaporator
m_b	Mass of the TEV bulb
$\dot{m}_{in}$	Mass flow rate of the refrigerant flowing into the evaporator
$\dot{m}_{out}$	Mass flow rate of the refrigerant flowing out of the evaporator
$\dot{m}_v$	Mass flow rate through the valve
P_b	Bulb pressure

P_c	Condenser pressure
P_e	Evaporator pressure
P_0	Assumed variable, ($P_0 = K_s x_0 / A$)
s_1, s_2	Normalizing parameters
TEV	Thermostatic Expansion Valve
T_{air}	Temperature of air
T_b	Bulb Temperature
T_{ero}	Temperature of refrigerant at evaporator outlet
T_r	Temperature of the refrigerant
T_w	Temperature of the evaporator wall
u_{eev}	Percentage opening of the EEV
V_k	Compressor volume
V_N	Error function
v_1, v_2, v_3	Valve parameters
x_0	Initial compression of the valve spring
δx	Displacement of expansion valve head

Greek symbols

α_0, α_1	Intermediate valve parameters
ρ_v	Density of refrigerant at valve inlet
τ_1, τ_2, τ_3	Bulb Parameters

η_k	Compressor volumetric efficiency
ρ_k	Density of refrigerant at compressor inlet
ρ	Coefficient of reflection
χ	Coefficient of expansion
γ	Coefficient of contraction
σ	Coefficient of shrinkage
ω	Compressor speed in rotations per second

TABLE OF CONTENTS

CHAPTER Page

LIST OF FIGURES

FIGURE Page

FIGURE Page

LIST OF TABLES

CHAPTER I

INTRODUCTION

The global demand for energy is ever increasing; a 44 % increase in energy demand is expected in the next twenty years [1]. Improving the efficiency of the energy consuming devices will play a crucial role in meeting the future energy needs. Heating, Venting, Air Conditioning and Refrigeration (HVAC) systems account for 40% of the commercial energy consumed in the US [2]. The availability of control oriented dynamic models of these systems can greatly help in the design and analysis of better control strategies, resulting in systems with higher efficiencies.

The vapor compression cycle is the most widely used method for Air-Conditioning and Refrigeration (AC&R) applications. Dynamic models have been developed for vapor compression system components that can accurately predict the behavior of the system if the mass flow rates to and from the heat exchangers are known accurately [3]. In particular, the two-phase flow dynamics are extremely sensitive to small variations in mass flow rate. The prediction of mass flow rate relies heavily on the empirical expansion valve and compressor parameters.

Traditionally, these empirical parameters have been estimated by employing expensive mass flow meters. But use of mass flow meters in every case is not possible which may lead to a badly tuned model. This research is motivated by the desire to find these empirical parameters on AC&R systems employing relatively low cost sensors like

---

This thesis follows the style of *IEEE Transactions on Control Systems Technology*.

temperature and pressure sensors.

In this study, the mathematical models of two commonly used expansion valves in AC&R systems, the Electronic Expansion Valve (EEV) and the Thermostatic Expansion Valve (TEV), are presented and analyzed. The parameters of the expansion valves and the compressor are estimated using nonlinear least squares and simplex search algorithms. Both of these algorithms are available in Matlab's Simulink Response Optimizer Toolbox [4]. The two algorithms are compared with each other with respect to speed and robustness.

In summary, this thesis addresses a unique challenge in the field of AC&R modeling. The remainder of this chapter is organized as follows. Section 1.1 presents the background on vapor compression cycle and the different components used in a vapor compression cycle. The literature review on TEV modeling and parameter estimation, along with evaporator modeling is presented in Section 1.2.

1.1 Background

1.1.1 Vapor Compression Cycle

There are four main components in a single-stage vapor compression system: a compressor, a condenser, an expansion valve and an evaporator. This system functions by transferring thermal energy from one heat exchanger to another through the circulation of a refrigerant. Figure 1.1 shows the basic components and the direction of refrigerant flow in an air conditioning unit, while Figure 1.2 shows the pressure vs. enthalpy diagram for a simple vapor compression cycle.

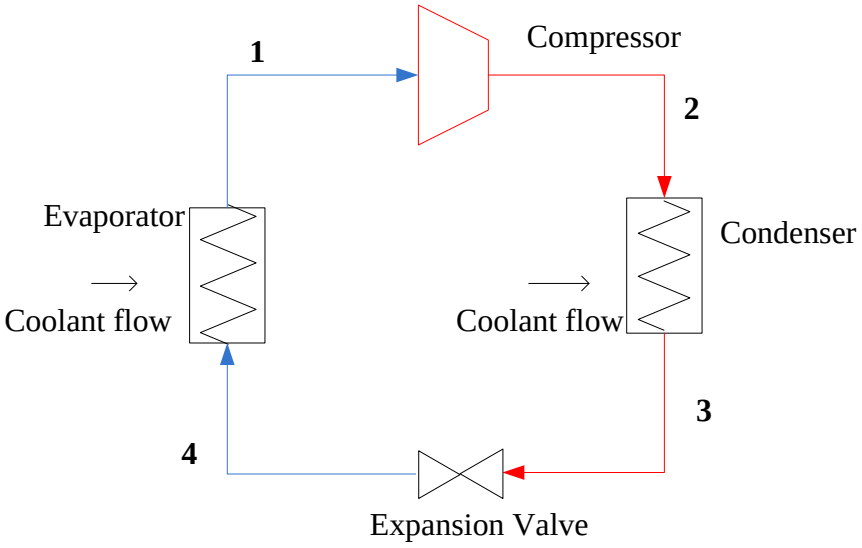

Fig. 1.1 Basic components of a vapor compression system

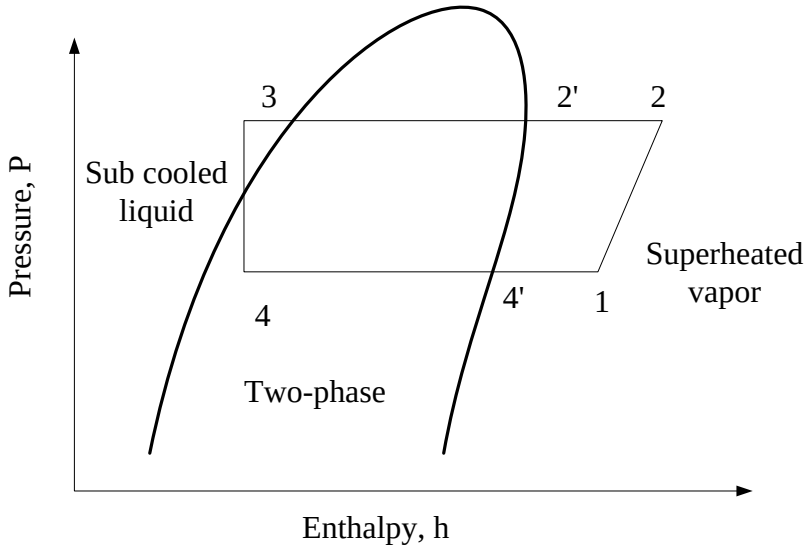

Fig. 1.2 P-h diagram of a vapor compression system

The operation of the vapor compression cycle occurs as follows. Starting at the compressor outlet (point 2), the refrigerant pumped out of the compressor is a single phase superheated vapor. This superheated vapor is circulated through the condenser and

gradually transfers its thermal energy to the external environment as it condenses. At the condenser exit (point 3), the refrigerant is typically a saturated or sub-cooled liquid. This liquid refrigerant expands and cools down as it passes from high pressure to low pressure region through the expansion valve (point 4); the refrigerant is a two phase fluid at this point. As the refrigerant travels through the evaporator, it absorbs thermal energy from the surroundings and its evaporates. At the exit of the evaporator (point 1), the refrigerant is typically a superheated vapor, due to the fact that liquid refrigerant that enters the compressor can cause extensive damage.

There are many types of expansion devices available in the market now, among which the Electronic Expansion Valve (EEV) and the Thermostatic Expansion Valve (TEV) are more popular. A brief overview of these expansion devices are given below. The detailed mathematical modeling of the expansion valves is given in Chapter II.

1.1.2 Electronic Expansion Valve

Electronic Expansion Valve is a relatively modern type of expansion valve used in AC&R systems. It consists of a needle valve controlled by a stepper motor. By controlling the stepper motor, the user can control the area of opening of this valve, thus controlling the pressure drop and the mass flow rate through the valve. A schematic of this type of valve is given in Figure 1.3 below.

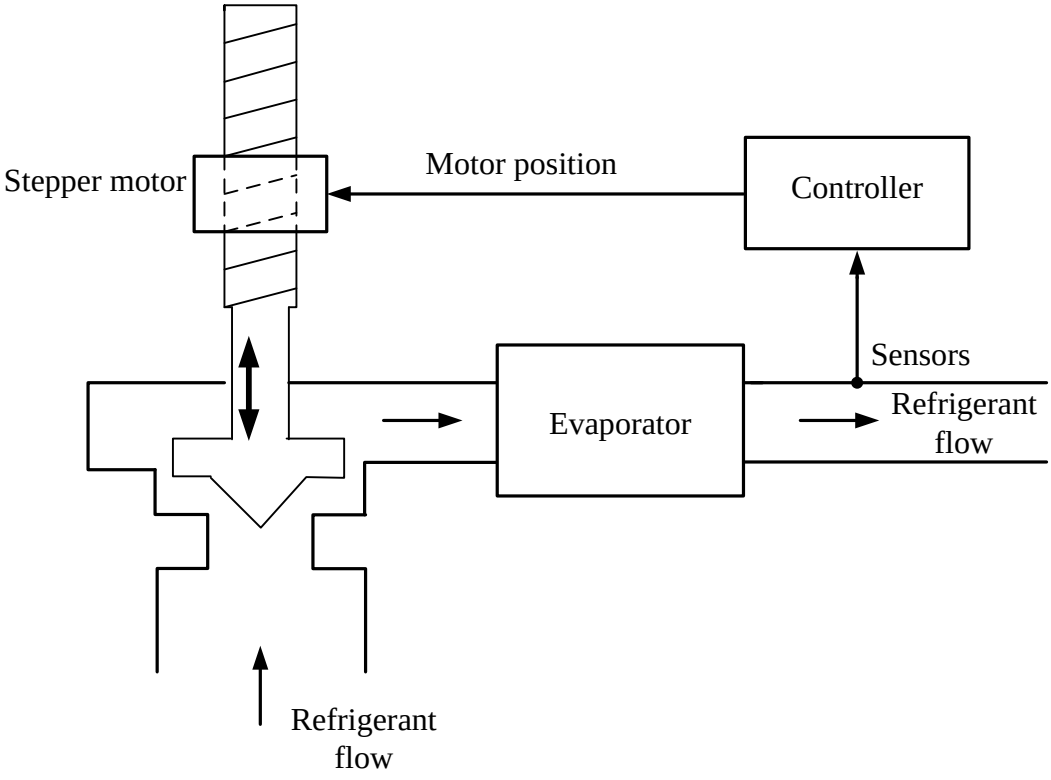

Fig. 1.3 Schematic representation of an EEV in operation

1.1.3 Thermostatic Expansion Valve

A Thermostatic Expansion Valve (TEV) regulates the amount of refrigerant entering the evaporator in a vapor compression system based on the superheat of the refrigerant at evaporator exit. TEV senses the superheat of the refrigerant at the evaporator exit using a bulb, filled with a two-phase fluid, attached to the tube wall at the evaporator exit. The bulb and the refrigerant at evaporator exit come into a thermal equilibrium.

As can be seen in Figure 1.4, a TEV consists of an expansion valve connected to a bulb filled with a refrigerant. At all operating conditions of the TEV, the refrigerant in the bulb is in the two-phase region. As the temperature increases (decreases), more (less)

of the fluid in the bulb is in vapor phase and the pressure due to vapor increases (decreases). This pressure is called the bulb pressure. Due to the presence of two-phase fluid in the bulb, the bulb pressure is very sensitive to the bulb temperature. The bulb pressure can be predicted by knowing bulb temperature and the thermodynamic properties of the refrigerant present in the bulb.

Figure 1.4 shows the forces acting on diaphragm of a TEV. The force caused by the bulb pressure is balanced by the spring force and force due to evaporator pressure. For example, if the temperature of the refrigerant at the evaporator exit increases while the pressure in the evaporator remains constant, the bulb temperature increases which in turn increases the bulb pressure. This increase in bulb pressure will exert a force that will try to open the expansion valve, thus increasing the mass flow rate of the refrigerant flowing into the evaporator, lowering the superheat.

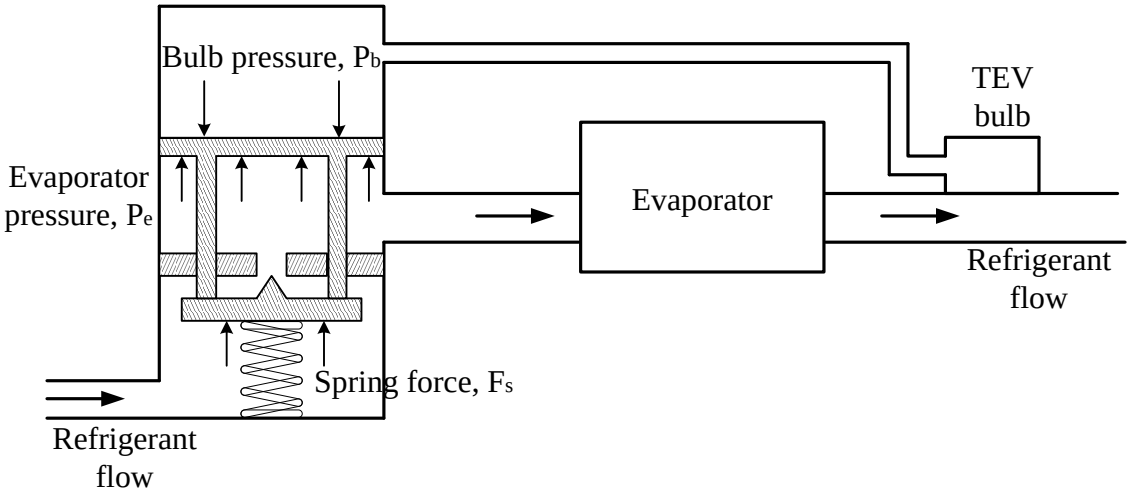

Fig. 1.4 Schematic representation of a TEV in operation

The minimum superheat required to open the expansion valve is called the static superheat or the offset temperature. The static superheat can be changed by changing the spring pretension. In most commercially available TEVs, this can be done by turning a knob which changes the initial displacement of the spring thereby varying its spring pretension.

Opening superheat is the difference between the actual refrigerant superheat and the static superheat. TEVs are generally designed such that the mass flow rate of the refrigerant through the valve is proportional to the opening superheat [5].

1.2 Literature Survey

1.2.1 Thermostatic Expansion Valve

Extensive literature is available on the different aspects of a TEV, mainly the mathematical model [5], [6], [7] and the hunting phenomenon [8], [9]. The mathematical model of the TEV mainly consists of the bulb model and the valve model.

One of the earliest works on vapor compression system modeling was done by [10]. The TEV model consisted of a differential equation relating the superheat to the mass flow rate through the expansion valve. It did not account for the different pressures acting on the diaphragm, hence was not able to predict rapid changes when encountered.

The TEV model was improved by representing the forces acting on the diaphragm in terms of temperature [6]. This can be done since the valve dynamics are much faster than the sensor dynamics. Sensor dynamics were modeled by a first order lag, and the time constant was assumed to be known. In [7] the mass flow rate through

the expansion valve is linearly related to the net pressure acting on the diaphragm of the valve. This model was combined with the orifice equation in [5] and it assumes a constant pressure difference across the valve. For varying pressure difference, the valve model is given in [11]. This equation is,

$$\dot{m}_v = C_d(P_b - P_e - P_0)\sqrt{\rho_v(P_c - P_e)} \tag{1.1}$$

The bulb model is found by applying the conservation of energy equation to the bulb and its contents. Since the bulb along with its contents, a two-phase substance, is difficult to model accurately, assumptions can be made to reduce the modeling complexity. In [5], the authors model the bulb with varying degrees of complexity. While most complex, one of the most accurate ways to model a bulb is to take a finite volume approach. Another approach, the model can be simplified by assuming the entire bulb to be a single unit, i.e. using the lumped capacitance approach. The simplest model for the bulb is to assume a first order lag for the bulb temperature. The authors [5] compare the results obtained by the different approaches and show that the lumped capacitance approach behaves almost similarly to the most accurate model.

Brorsen and Ten-napel [12] estimate the parameters associated with the transfer function model of a TEV bulb by attaching the TEV bulb to a copper tube carrying thermally controlled water. By changing the temperature of water, the TEV bulb's temperature is controlled, which in turn controls the valve opening. This drawback of this approach is that only the TEV bulb dynamics are studied.

1.2.2 Evaporator Modeling

The early evaporator models were spatially independent simple lumped parameter models [13], [14], [15], [16]. These models could be used for finding the average refrigerant properties but were not so helpful to find superheat or the exact temperature at the inlet and exit of the evaporator. MacArthur and Grald [17] developed a spatially dependent model based on the conservation of mass, momentum and energy. This unsteady two-phase model was expressed as partial differential equations. This model was quite accurate; However due to the complexity of the model it was not used for control applications.

Wedekind's [18] work on mean void fraction (the volumetric ratio of vapor to the total volume) resulted in greatly simplifying the spatially dependent evaporator models. He showed that the mean void fraction in the evaporator remains approximately the same during most operating conditions. Thus the liquid-vapor distribution in the two-phase region of the evaporator can be described by just one variable, the mean void fraction.

The time invariant mean void fraction was used to simplify the partial differential equations to ordinary differential equations in [3]. This moving boundary evaporator model ignores the pressure drop across the evaporator. This model is accurate for all simple heat exchanger configurations. The nonlinear ordinary differential equations were linearized in [19]. The use of moving boundary models can be seen in [20], [21], [22] and [23].

1.3 Organization of the Thesis

The remainder of this dissertation is organized as follows. Chapter II presents the modeling of the expansion valves, the compressor and the evaporator. Chapter III details the experimental set ups used. Chapter IV gives an overview of the parameter estimation methods and the Simulink Response Optimization toolbox. Chapter V describes the procedure followed for parameter estimation of the expansion valve and compressor parameters followed by the results obtained. Chapter VI deals with the conclusion and the future scope of this research work.

CHAPTER II

MODELING

This chapter discusses the modeling and model validation of the expansion valves (EEV & TEV), compressor and a heat exchanger (evaporator).

2.1 Electronic Expansion Valve

The Electronic Expansion Valve can be modeled by the orifice equation [24], as shown in Eq. (2.1). A_v, is the area of orifice opening and C_d is the coefficient of discharge of the expansion valve at that specific condition. Coefficient of discharge is a dependent on the EEV geometry and the thermal–fluid properties of the refrigerant flowing through the valve [25]. This quantity can be assumed to be a constant over a small operating condition and the area of opening of the expansion valve is assumed to be linear over a small operating region. These two assumptions have been used to obtain Eq. (2.2). The dynamics of the heat exchangers in a Vapor compression system are much slower than the dynamics of the valve; hence a static algebraic expression is used to model the area of opening of the valve as a function of the EEV opening.

$$\dot{m}_v = C_d A_v \sqrt{(P_c - P_e)\rho_v} \tag{2.1}$$

$$\dot{m}_v = (v_1 + v_2 u_{eev})\sqrt{(P_c - P_e)\rho_v} \tag{2.2}$$

2.2 Thermostatic Expansion Valve

The TEV model is essentially two system models, the TEV bulb and the valve model. A schematic representation of a TEV is given in Figure 1.4. The TEV model derived in this section is valid for both internally and externally equalized TEVs. The following assumptions are made for the TEV model:

1. The refrigerant present in the bulb of the TEV as well as its thermodynamic properties are known.
2. The spring is linear in the operating range, a valid assumption considering the very minute net displacement of the spring during operation.

Lumped capacitance method is used to model the TEV bulb [26].

$$h_o A_o (T_{air} - T_b) - h_{rb} A_{rb} (T_b - T_{ero}) = m_b C_b \left(\frac{dT_b}{dt}\right) \tag{2.3}$$

The Laplace transform of the above equation gives,

$$T_b(s) = \frac{\tau_1 T_{air}(s) + \tau_2 T_{ero}(s)}{s + \tau_1 + \tau_2} \tag{2.4}$$

If the heat transfer between the bulb and the outside environment is neglected then the Laplace transform of Eq. (2.3) is,

$$\frac{T_b(s)}{T_{ero}(s)} = \frac{1}{1 + \tau_3 s} \tag{2.5}$$

The bulb pressure is the saturation pressure of the refrigerant in the bulb, $P_b = P_{sat}(T_b)$. The force balance on the diaphragm of the expansion valve is given by,

$$P_b A_1 = P_e A_2 + K_s (x_0 + \delta x) \tag{2.6}$$

where, x_0, is the initial compression of the spring and δx, is the net axial movement of the valve head. Let us define, $P_0 = \frac{K_s x_0}{A_2}$. Eq. (2.6) can be written as,

$$\delta x = \frac{(P_b)A_1 - (P_e - P_0)A_2}{K_s} \tag{2.7}$$

Near a particular operating condition the area of the valve opening is directly proportional to the displacement of the valve head. Hence,

$$A_v = \alpha(x_0 + \delta x) \tag{2.8}$$

Using Eq. (2.7) and (2.8)

$$A_v = \alpha_0 P_b - \alpha_1(P_e + P_0) \tag{2.9}$$

Combining the above equations with the equation of flow through an orifice one can obtain the equation for the mass flow rate with respect to the bulb pressures and other parameters.

$$\dot{m}_v = (v_1 + v_2 P_b + v_3 P_e)\sqrt{\rho_v(P_c - P_e)} \tag{2.10}$$

Eq. (2.5) and (2.10) represent the mathematical model of the TEV. The parameters that need to be identified in this model are $\tau_3, v_1, v_2 \; and \; v_3$. . Once these parameters have been estimated the mass flow rate of the refrigerant through the expansion valve can be known. In this derivation the area of the application of bulb and evaporator pressure is assumed to be different. If the area of application of force is same then Eq. (2.10) can be reduced to,

$$\dot{m}_v = (v_1 + v_2(P_b - P_e))\sqrt{\rho_v(P_c - P_e)} \tag{2.11}$$

2.3 Compressor

The variable speed compressor is modeled by the following equations:

$$\dot{m}_k = \eta_v \omega V_k \rho_k \tag{2.12}$$

$$\eta_v = k_1 - k_2(P_c/P_e) \tag{2.13}$$

Since at higher operating speeds and higher pressure ratios there will be more leakage the volumetric efficiency was defined keeping that in mind. In case of a constant speed compressor or when the volume of the compression chamber is not known these terms could be combined with the unknowns.

2.4 Evaporator

Moving boundary approach is used to model the evaporator. This approach was chosen over the finite control volume approach [27] due to its better computational speed and less complexity of the model.

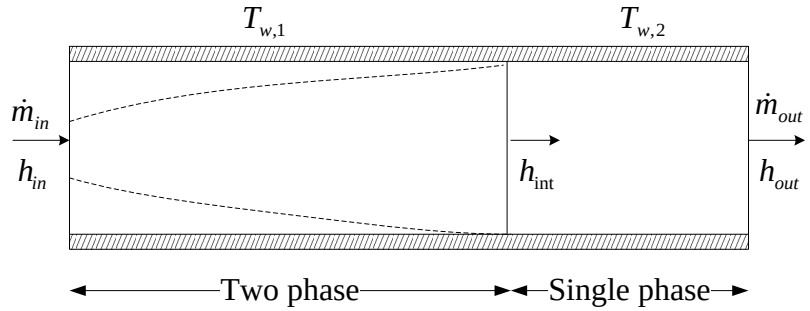

Fig. 2.1 MB Evaporator model diagram

In this approach the heat exchanger is split into different regions according to the fluid phases existing in it and the boundary separating the different regions is time varying. In case of the evaporator, there are two regions, the two phase region and the

superheated vapor region as shown in Figure 2.1. There are several assumptions that are made while modeling the evaporator using this approach. They are:

1. Even if the evaporator geometry is not simple, it is represented as a simple thin tube with equivalent mass, length, surface area and volume.
2. The refrigerant flow along the evaporator is modeled as a one dimensional fluid flow.
3. Axial heat conduction in the refrigerant is negligible.
4. Pressure drop across the evaporator is negligible.
5. Viscous dissipation of energy is negligible.

The conservation of refrigerant mass (2.14), refrigerant energy (2.15) and wall energy (2.16) equations are solved over the two phase and superheated regions to obtain the dynamic evaporator model. Conservation of momentum equation is not used due to the assumption of negligible pressure drop in the evaporator.

$$\frac{\partial \rho A}{\partial t} + \frac{\partial \dot{m}}{\partial z} = 0 \qquad (2.14)$$

$$\frac{\partial (\rho A h - A P)}{\partial t} + \frac{\partial (\dot{m} h)}{\partial z} = p_i \alpha_i (T_w - T_r) \qquad (2.15)$$

$$(C_p \rho A)_w \frac{\partial T_w}{\partial t} = p_i \alpha_i (T_r - T_w) + p_o \alpha_o (T_a - T_w) \qquad (2.16)$$

A detailed derivation of the above partial differential equations can be found in [17]. The nonlinear ordinary differential equations are obtained by integrating the above

partial differential equations over each fluid region. The integration equation used is given in Eq. 2.17. The integration over a fluid region was made possible by assuming lumped parameters in each fluid region. Eq. 2.18 was used to obtain a single air temperature over the length of the evaporator. Eq. 2.19 was used to obtain average density in the two phase region. Here $\bar{\gamma}$, is the mean void fraction (ratio of vapor volume over total volume in the two-phase region) in the two-phase region. As mentioned in the literature review, the mean void fraction over the operating range of the evaporator can be considered to be a constant [18].For this research the mean void fraction is calculated using Zivi's correlation [28].

$$\int_{z_1(t)}^{z_2(t)} \frac{\partial f(z,t)}{\partial t}\, dz = \frac{d}{dt}\int_{z_1(t)}^{z_2(t)} f(z,t)dz - f(z_2(t),t)\frac{dz_2(t)}{dt} + f(z_1(t),t)\frac{dz_1(t)}{dt} \quad (2.17)$$

$$T_a = T_{a,in}(\mu) + T_{a,out}(1-\mu) \quad (2.18)$$

$$\rho_1 = \rho_f(1-\bar{\gamma}) + \rho_g(\bar{\gamma}) \quad (2.19)$$

The other average properties used in the two-phase region are the enthalpy, $h_1 = \frac{(h_{in}+h_g)}{2}$ and quality of the refrigerant, $x = \frac{x_{in}+1}{2}$. The average properties used in the superheated region are the enthalpy, $h_2 = \frac{h_g+h_{out}}{2}$; Temperature of the refrigerant, $T_{r2} = T(P_e, h_2)$; Density of the refrigerant, $\rho_2 = \rho(P_e, h_2)$. Wattelet's correlation [29] is used to calculate the two-phase heat transfer between the refrigerant and the evaporator tubes, while, Gnielinski's correlation [30] is used to calculate the single-phase heat transfer. Both these correlations are valid for both R134a and R410A refrigerants.

The governing ordinary differential equations for the evaporator are given by Eq. 2.20-2.25

Conservation of refrigerant mass

$$\left(\frac{d\rho_f}{dP_e}(1-\bar{\gamma})+\frac{d\rho_g}{dP_e}(\bar{\gamma})\right)A_{cs}L_1\dot{P}_e+(\rho_f-\rho_g)(1-\bar{\gamma})A_{cs}\dot{L}_1 = \dot{m}_{in}-\dot{m}_{int} \tag{2.20}$$

$$\left[\left(\frac{\partial\rho_2}{\partial P_e}\Big|_{h_2}\right)+\frac{1}{2}\left(\frac{\partial\rho_2}{\partial h_2}\Big|_{P_e}\right)\left(\frac{dh_g}{dP_e}\right)\right]AL_2\dot{P}_e+\frac{1}{2}\left(\frac{\partial\rho_2}{\partial h_2}\Big|_{P_e}\right)AL_2\dot{h}_{out}+(\rho_g-\rho_2)A\dot{L}_1=\dot{m}_{int}-\dot{m}_{out} \tag{2.21}$$

Conservation of refrigerant energy

$$\left(\frac{d\rho_f h_f}{dP_e}(1-\bar{\gamma})+\frac{d\rho_g h_g}{dP_e}(\bar{\gamma})-1\right)A_{cs}L_1\dot{P}_e+(\rho_f h_f-\rho_g h_g)(1-\bar{\gamma})A_{cs}\dot{L}_1 = \dot{m}_{in}h_{in}-\dot{m}_{int}h_{int}+\alpha_{i1}A_i\left(\frac{L_1}{L_{total}}\right)(T_{w1}-T_{r1}) \tag{2.22}$$

$$\left[\left(\left(\frac{\partial\rho_2}{\partial P_e}\Big|_{h_2}\right)+\frac{1}{2}\left(\frac{\partial\rho_2}{\partial h_2}\Big|_{P_e}\right)\left(\frac{dh_g}{dP_e}\right)\right)h_2+\left(\frac{1}{2}\right)\left(\frac{dh_g}{dP_e}\right)\rho_2-1\right]AL_2\dot{P}_e+\frac{1}{2}\left[\left(\frac{\partial\rho_2}{\partial h_2}\Big|_{P_e}\right)h_2+\rho_2\right]AL_2\dot{h}_{out}+(\rho_g h_g-\rho_2 h_2)A_{cs}\dot{L}_1 = \dot{m}_{int}h_{int}-\dot{m}_{out}h_{out}+\alpha_{i2}A_i\left(\frac{L_2}{L_{total}}\right)(T_{w2}-T_{r2}) \tag{2.23}$$

Conservation of wall energy

$$(C_p\rho V)_w\dot{T}_{w1} = \alpha_{i1}A_i(T_{r1}-T_{w1})+\alpha_o A_o(T_a-T_{w1}) \tag{2.24}$$

$$(C_p\rho V)_w\left[\dot{T}_{w2}-\left(\frac{T_{w2}-T_{w1}}{L_2}\right)\dot{L}_1\right] = \alpha_{i2}A_i(T_{r2}-T_{w2})+\alpha_o A_o(T_a-T_{w2}) \tag{2.25}$$

The equations 2.20- 2.23 are algebraically combined to eliminate $\dot{m}_{int}$. The resulting equations represent the nonlinear evaporator model, Eq. 2.26. It is of the form, $Z(x,u)\,\dot{x}=f(x,u)$ with states, $x=[\,L_1 \quad P_e \quad h_{out} \quad T_{w1} \quad T_{w2}\,]^T$. The elements of the Z matrix are given in Table 2.1.

$$\begin{bmatrix} z_{11} & z_{12} & 0 & 0 & 0 \\ z_{21} & z_{22} & z_{23} & 0 & 0 \\ z_{31} & z_{32} & z_{33} & 0 & 0 \\ 0 & 0 & 0 & z_{44} & 0 \\ z_{51} & 0 & 0 & 0 & z_{55} \end{bmatrix} \begin{bmatrix} \dot{L}_1 \\ \dot{P}_e \\ \dot{h}_{out} \\ \dot{T}_{w1} \\ \dot{T}_{w2} \end{bmatrix} = \begin{bmatrix} \dot{m}_{in}(h_{in} - h_g) + \alpha_{i1} A_i \left(\frac{L_1}{L_{total}}\right)(T_{w1} - T_{r1}) \\ \dot{m}_{out}(h_g - h_{out}) + \alpha_{i2} A_i \left(\frac{L_2}{L_{total}}\right)(T_{w2} - T_{r2}) \\ \dot{m}_{in} - \dot{m}_{out} \\ \alpha_{i1} A_i (T_{r1} - T_{w1}) + \alpha_o A_o (T_a - T_{w1}) \\ \alpha_{i2} A_i (T_{r2} - T_{w2}) + \alpha_o A_o (T_a - T_{w2}) \end{bmatrix} \quad (2.26)$$

Table 2.1 Matrix Elements of $\boldsymbol{Z(x,u)}$ for the nonlinear evaporator model

z_{11}	$\big(\rho_f(h_f - h_g)\big)(1-\bar{\gamma})A_{cs}$
z_{12}	$\left(\left(\frac{d\rho_f h_f}{dP_e} - \frac{d\rho_f}{dP_e}h_g\right)(1-\bar{\gamma}) + \left(\frac{d\rho_g h_g}{dP_e} - \frac{d\rho_g}{dP_e}\right)(\bar{\gamma}) - 1\right)A_{cs}L_1$
z_{21}	$\rho_2\big(h_g - h_2\big)A_{cs}$
z_{22}	$\left[\left(\left(\frac{\partial\rho_2}{\partial P_e}\Big\vert_{h_2}\right) + \frac{1}{2}\left(\frac{\partial\rho_2}{\partial h_2}\Big\vert_{P_e}\right)\left(\frac{dh_g}{dP_e}\right)\right)(h_2 - h_g) + \left(\frac{1}{2}\right)\left(\frac{dh_g}{dP_e}\right)\rho_2 - 1\right]A_{cs}L_2$
z_{23}	$[\frac{1}{2}\left(\frac{\partial\rho_2}{\partial h_2}\Big\vert_{P_e}\right)(h_2 - h_g) + \left(\frac{\rho_2}{2}\right)]A_{cs}L_2$
z_{31}	$\big[(\rho_g - \rho_2) + (\rho_f - \rho_g)(1-\bar{\gamma})\big]A_{cs}$
z_{32}	$\left[\left[\left(\left(\frac{\partial\rho_2}{\partial P_e}\Big\vert_{h_2}\right) + \frac{1}{2}\left(\frac{\partial\rho_2}{\partial h_2}\Big\vert_{P_e}\right)\left(\frac{dh_g}{dP_e}\right)\right)\right]L_2 + \left[\left(\frac{d\rho_f}{dP_e}\right)(1-\bar{\gamma}) + \left(\frac{d\rho_g}{dP_e}\right)(\bar{\gamma})\right]L_1\right]A_{cs}$
z_{33}	$\frac{1}{2}\left(\frac{\partial\rho_2}{\partial h_2}\Big\vert_{P_e}\right)A_{cs}L_2$

Table 2.1 Continued

z_{44}	$\left(C_p \rho V\right)_w$
z_{51}	$\left(C_p \rho V\right)_w \left(\frac{T_{w1} - T_{w2}}{L_2}\right)$
z_{55}	$\left(C_p \rho V\right)_w$

For the purposes of parameter estimation, linearized moving boundary model is preferred over the nonlinear evaporator model due to its higher computational speed. The nonlinear ordinary differential equations are linearized over an operating point to get the linearized evaporator model as shown below.

$$\dot{x} = Z(x,u)^{-1} f(x,u) \tag{2.27}$$
$$= h(x,u)$$

Using Taylor's series expansion, $x = x_0 + \delta x,$ neglecting the higher order term, Eq. 2.27, can be written as,

$$\delta\dot{x} = \left[\left.\frac{\partial h}{\partial x}\right|_{x_0,u_0}\right]\delta x + \left[\left.\frac{\partial h}{\partial u}\right|_{x_0,u_0}\right]\delta u \tag{2.28}$$

$$A_e = \left[\left.\frac{\partial h}{\partial x}\right|_{x_0,u_0}\right];\ B_e = \left[\left.\frac{\partial h}{\partial u}\right|_{x_0,u_0}\right] \tag{2.29}$$

The linearized evaporator model thus is, $\dot{\delta x} = A_e \delta x + B_e\ \delta u.$ The inputs $= [u - u_0].$ $u = \left[\dot{m}_{in} \quad \dot{m}_{out} \quad h_{in} \quad T_{a,in} \quad \dot{m}_a\right]^T$. The elements of the linearized evaporator model are given in the Appendix for quick reference. The detailed derivation

of A_e, B_e can be found in [19]. This linearized model is used in the subsequent chapters for parameter estimation.

CHAPTER III

EXPERIMENTAL SYSTEM

Two experimental set ups were used to test the parameter estimation algorithms. One test rig is a custom instrumented 3-Ton air conditioning unit from Trane. This system is shown in Figure 3.1. In this system, an EEV from Parker is used as the expansion valve. The compressor is a two-stage constant speed scroll compressor. The mass flow rate of the air over the evaporator and condenser coils can be independently adjusted by varying the evaporator and condenser fan speeds respectively. The refrigerant used is R410A. The schematic diagram of this experimental set up is shown in Figure 3.2. List of all the important components used in this experimental system is given in Table 3.1.

The second test rig is a custom designed refrigeration system with water as the secondary coolant. The experimental set up is shown in Figure 3.3. The system is designed such that it is possible to use either the EEV or the TEV as the expansion valve. It has a variable speed scroll compressor. The secondary coolants flow rate over the evaporator coils is controlled by using a variable flow rate valve. The refrigerant used is R134a. A schematic diagram of the refrigerant loop of this experimental set up is given in Figure 3.4. Further details about this system can be found in [31]. List of important components used in this experimental system is given in Table 3.2.

Fig. 3.1 3-Ton residential air conditioner from Trane

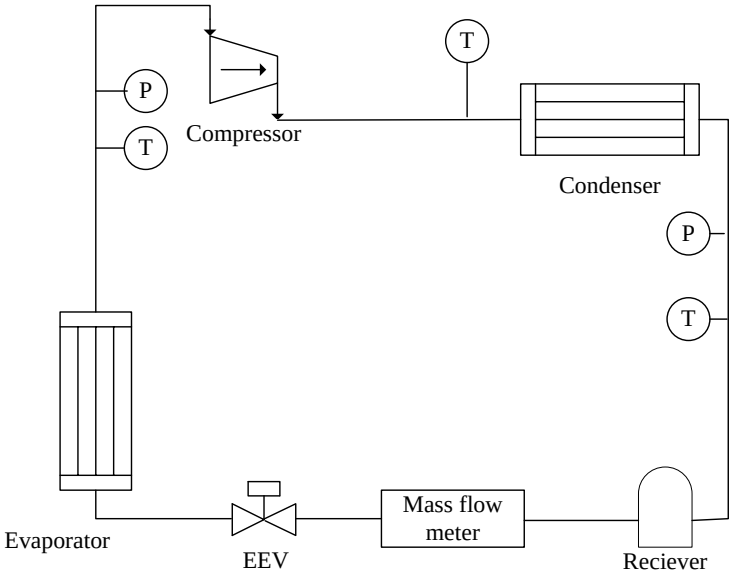

P - Pressure sensor
T - Thermocouple

Fig. 3.2 Schematic diagram of the residential air conditioner

Table 3.1 Component details of the Experimental Setup (Residential air conditioner)

Component	**Manufacturer**	**Model Number**
Air Conditioning System	Trane	XL 16i
EEV	Parker	020432-00
Thermocouple	Omega	GTMQSS-062U-6
Pressure sensor	Omega	PX309-500G5V
Mass flow meter	McMillan	102 Range 8
Data Acquisition Board	Measurement Computing	PCI-DAS6071
DAQ software	National Instruments	Labview

Table 3.2 Component details of the Experimental Setup (Water chiller system)

Component	**Manufacturer**	**Model Number**
Air Conditioning System	Custom built	
EEV	Sporlan Valve Co.	SEI 0.5-10 -S
TEV	Parker	46 JW
Compressor	MasterFlux	Sierra 03-0982Y3
Thermocouple	Omega	GTMQSS-062U-6
Pressure sensor	Cole-Parmer	07356-04
Mass flow meter	McMillan	102 Range 5
DAQ software	Quanser	WinCon 5.0

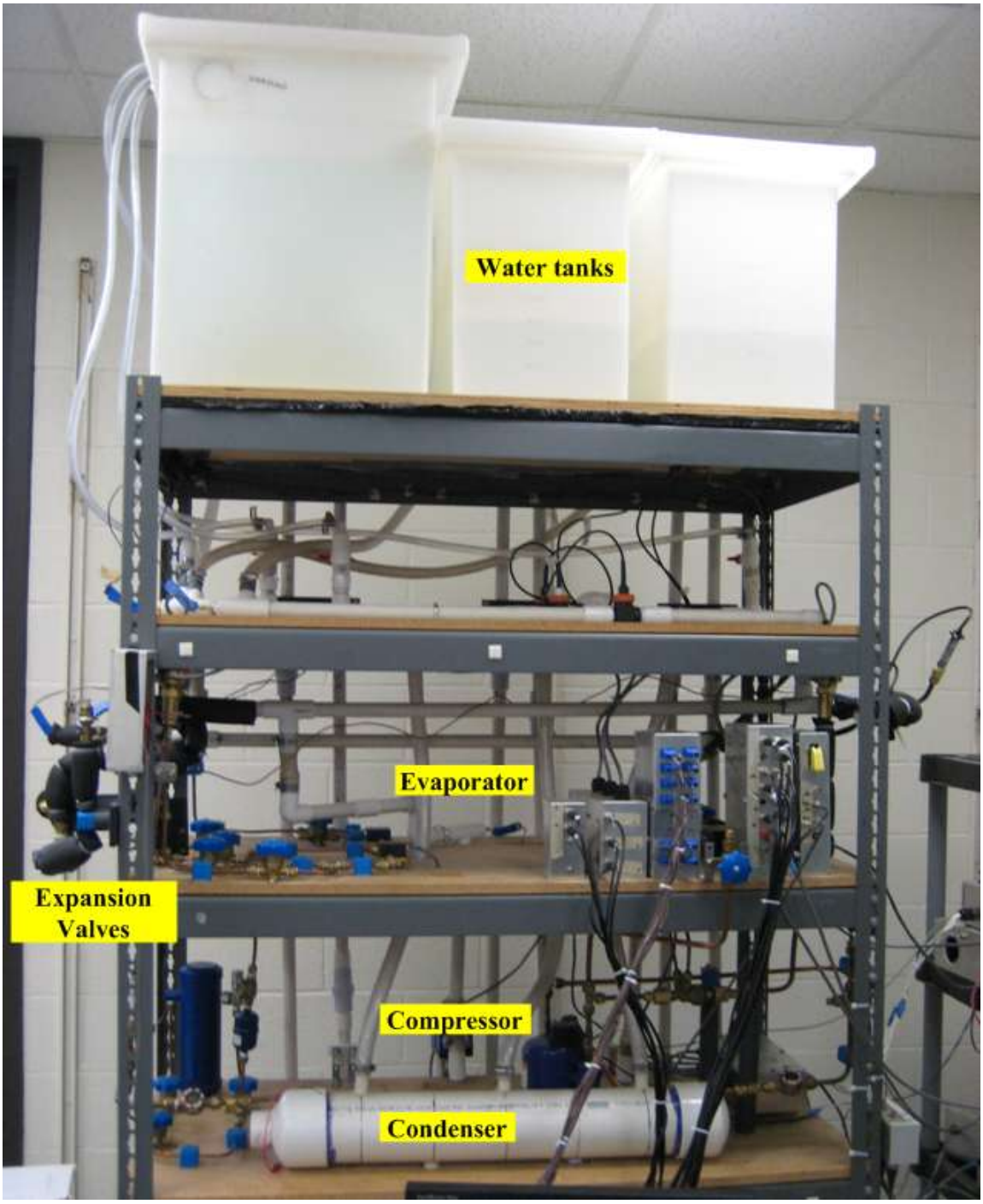

Fig. 3.3 0.5 Ton water chiller system

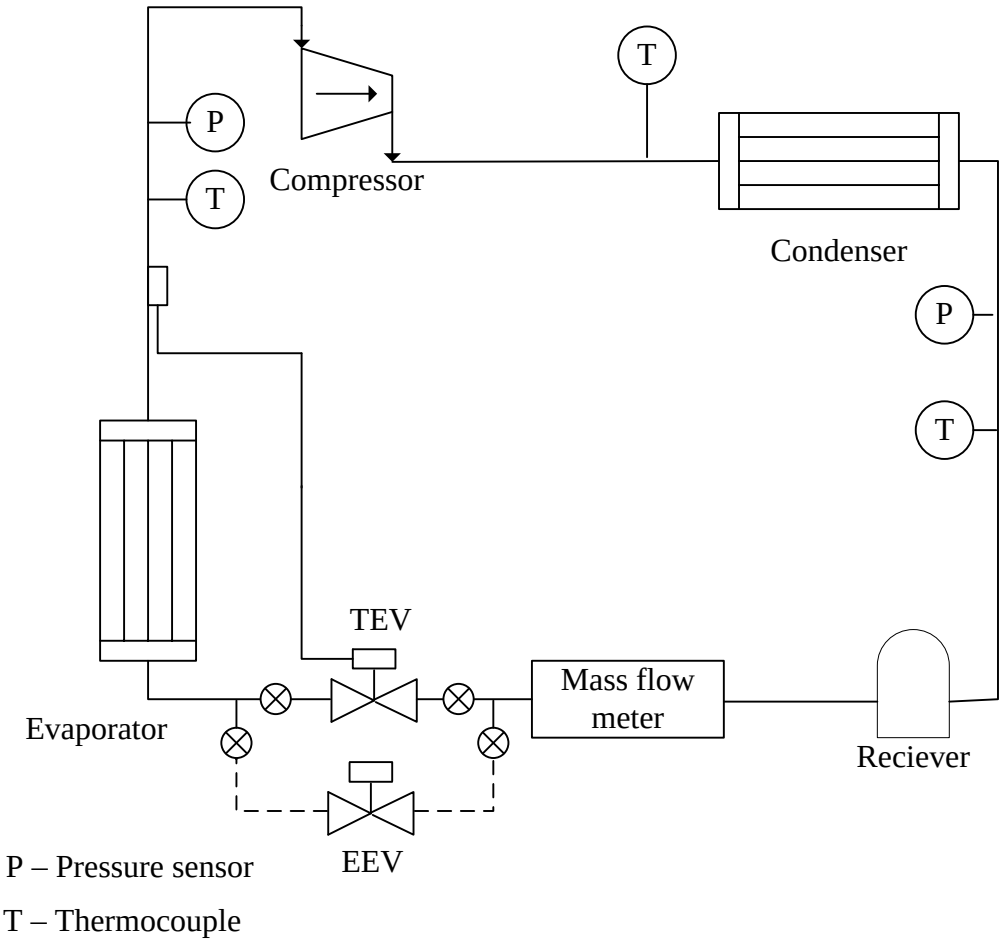

Fig. 3.4 Schematic diagram of the water chiller system

CHAPTER IV

PARAMETER ESTIMATION

A parameter estimation algorithm is required to identify the valve and compressor parameters so that the vapor compression cycle model can mimic the actual AC&R plant. A parameter estimation algorithm identifies the unknown parameters of a given grey box model by minimizing the error between the model output and the plant output, when both the plant and the model is given the same input [32]. Eq. (4.1) gives the quadratic error between the model and plant. This value needs to be minimized to estimate the unknown parameters.

$$V_N(\theta) = \sum_{i=1}^{N} \left(y(t) - \hat{y}(t|\theta)\right)^2 \tag{4.1}$$

Parameter estimation methods can be divided into two classes, based on how the error, V_N, is minimized. One is the analytical method and the other being the numerical search method. Figure 4.1 mentions some of the most common parameter estimation methods and their type. Analytical methods are preferred over the numerical search techniques due to their higher computational speeds and simplicity of the algorithm [32], [33].

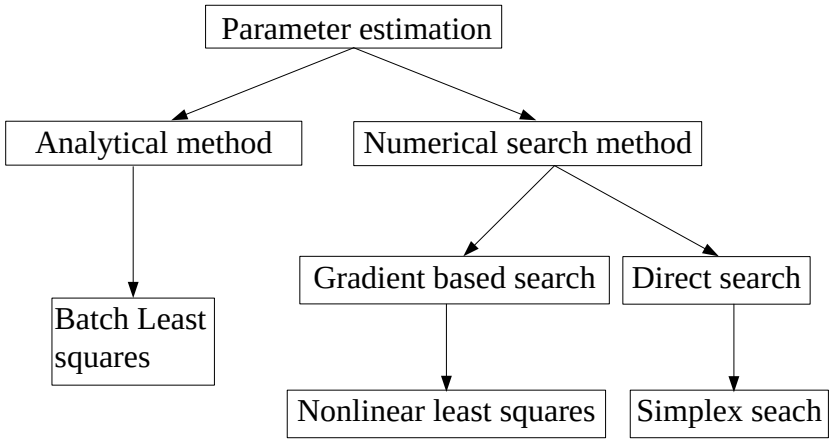

Fig. 4.1 Common parameter estimation methods and their types

4.1 Batch Least Squares

Batch least squares or commonly known as least squares algorithm was proposed by Karl Friedrich Gauss and he used it to estimate the orbits of different planets and asteroids. This algorithm is often used for parameter estimation. It is simple to use this algorithm on a mathematical model given in Eq. 4.2.

$$y(t) = a_1\, y(t-1) + \ a_2\, y(t-2) + .. + a_n y(t-n) + \ b_1\, u(t-1) + b_2 u(t-2) + .. + \ b_n u(t-m) \tag{4.2}$$

Writing the above equation in a compact form,

$$\theta = [a_1, a_2, \ldots a_n\ , b_1, b_2, \ldots\ b_m]^T \tag{4.3}$$

$$\phi(t) = [y(t-1), y(t-2), \ldots y(t-n), u(t-1), u(t-2), \ldots u(t-m)]^T \tag{4.4}$$

Eq. (4.2) can be written as $y(t) = \phi^T(t)\theta$, 'y' is the observation, 'u' is the input and 'θ' is the unknown parameter vector. According to the least squares method the best estimate of the unknown parameter is given by,

$$\hat{\theta}_N = [\sum_{t=1}^{N} \phi(t)\phi^T(t)]^{-1} \sum_{t=1}^{N} \phi(t)y(t) \quad (4.5)$$

If the mathematical model is not in the form given in Eq. (4.2), as in the case of this research, it can be converted to this form as shown in [32]. Initially, the least squares technique was used to estimate the valve and compressor parameters. The system is excited by changing the valve opening as can be seen in Figure 4.2. The estimated mass flow rate of the refrigerant at valve inlet is compared with the measured flow rate in Figure 4.3. It can be clearly seen that the estimation technique has failed. The estimates of the EEV and compressor parameter calculated using least squares technique is tabulated in Table 4.1.

Table 4.1 EEV and compressor model parameter estimation using least squares

Estimation method	EEV Parameters		Compressor Parameters		RMS error in mass flow rate at valve (grams/second)
	v_1	v_2	k_1	k_2	
Using mass flow measurements	-3.20	0.78	1.07	0.07	0.095
Batch least squares	-12.36	0.90	-0.01	0.01	6.783

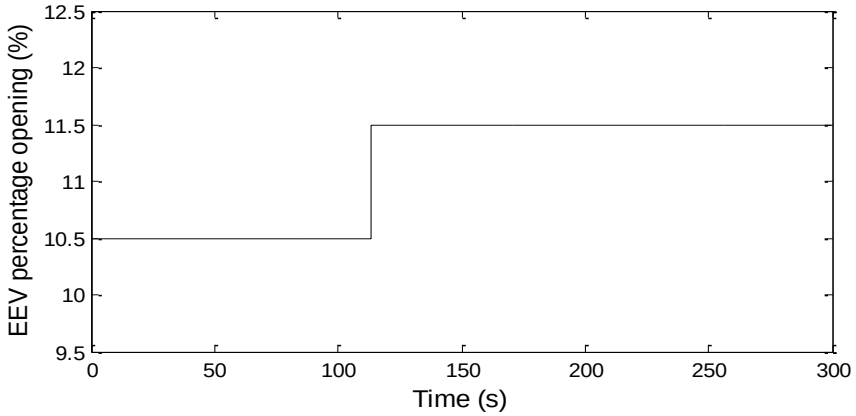

Fig. 4.2 System excited by stepping the EEV

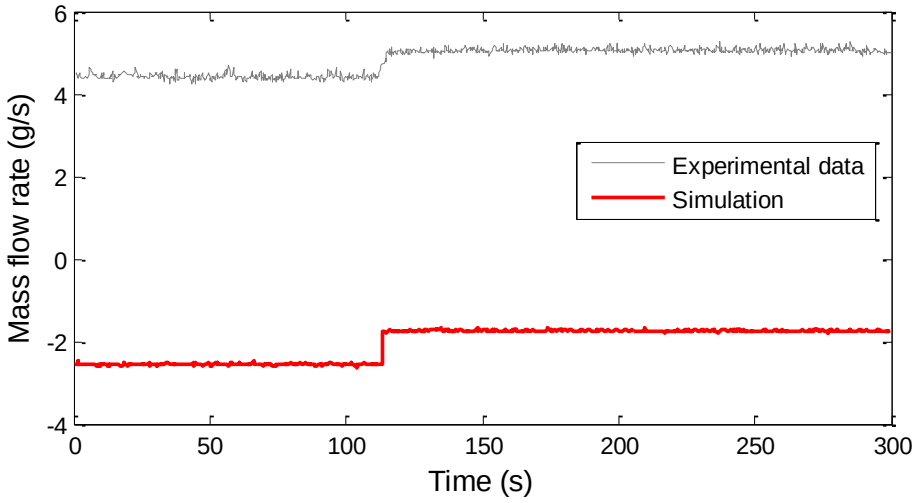

Fig. 4.3 Comparison of measured and simulated mass flow rate of the refrigerant at the valve inlet

The reason for the failure of least squares approach is thought to be codependency between the valve and compressor parameters. Least squares technique fails to minimize functions of the type given by Eq. 4.6 or 4.7 [15].

$$V_N = \sum_{t=1}^{N} l(\varepsilon(t,\theta),\theta) \tag{4.6}$$

$$V_N = \sum_{t=1}^{N} \zeta(t,\theta)\, \alpha(\varepsilon(t,\theta)) \tag{4.7}$$

For such cases parameter estimation is only possible using iterative numerical search techniques [34]. Figure 4.4 graphically represents the iterative numerical search algorithm.

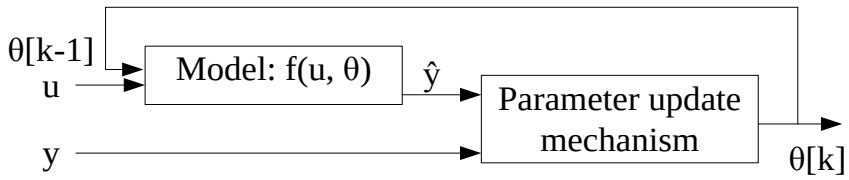

Fig. 4.4 Graphical representation of a generic parameter estimation using numerical search algorithm

Based on the parameter update mechanism, numerical search methods can be divided into two types, gradient based search and direct search. In this thesis, both these types of numerical search techniques are discussed.

4.2 Nonlinear Least Squares

A common numerical search algorithm used for parameter estimation in grey box models is the nonlinear least squares [35]. It is a type of gradient based numerical search method that makes use of the model information while computing the estimate. The use of nonlinear least squares for parameter estimation can be found in [36] and [37].

The basic iterative parameter update scheme of nonlinear least squares algorithm is [32]:

$$\hat{\theta}^{i+1} = \hat{\theta}^{i} - \mu_i R_i^{-1} \hat{g}_i \tag{4.8}$$

Here $\hat{\theta}^{i}$ is the parameter estimate after iteration number *i*. The search scheme is thus made up of the three entities μ_i, R_i and $\hat{g}_i$. μ_i is the step size, $\hat{g}_i$ is an estimate of the gradient $V'_N(\hat{\theta}^{i})$ and R_i is the matrix that modifies the search direction. The step size, μ_i, is chosen such that, $V_N(\hat{\theta}^{(i+1)}) < V_N(\hat{\theta}^{(i)})$. A simple choice of the search

direction, R_i, is to take it to be the identity matrix. This approach is known to be inefficient as the error function reaches its minimum. One way to overcome this problem is to use Eq. 4.9 to compute the search direction.

$$R_i = \sum_{t=1}^{N}\left(\psi(t,\theta_i)\,\psi^T(t,\theta_i)\right) + \lambda I \tag{4.9}$$

In the above equation, $\psi(t,\theta_i)$, is the gradient matrix of $\hat{y}$ with respect to θ, and λ is a positive scalar.

4.3 Simplex Search

Simplex search algorithm is a commonly used non-gradient based numerical search method [38] and [39]. This technique was proposed by John Nelder and R. Mead in 1965 [40]. This search method is also called the Nelder-Mead method or the amoeba method. The use of simplex search for parameter estimation can be found in [41] and [42]. The advantage of simplex search is that since it does not compute gradients it is comparatively faster than nonlinear least squares algorithm, but is less robust, that is, it is more prone to settle at a local minima.

Simplex search algorithm uses the concept of simplex to minimize the error between the model and actual plant outputs. Simplex can be defined as the smallest convex set of given points. For example in a single dimensional space, a line segment is the simplex. The line segment is also called the 1- simplex. N-simplex is an n-dimensional polytope with n+1 vertices. Thus, 2-simpex is a triangle and 3-simplex is a tetrahedron.

Simplex search algorithm uses a simplex of n+1 vertices for a problem having n unknown parameters. The algorithm first makes a simplex around the initial guess, x_0, by adding a small constant percentage of each component to x_0. Thus the n+1 vertices of the initial simplex are these n points in the n-dimensional space and the initial guess value.

Four scalar parameters must be defined before running this search method. They are the coefficients of reflection (ρ), expansion, (χ), contraction (γ), and shrinkage (σ). These parameters should satisfy

$$\rho > 0, \quad \chi > 1, \quad \chi > \rho, \quad 0 < \gamma < 1, \quad and \quad 0 < \sigma < 1 \tag{4.10}$$

While any parameter values satisfying the above conditions will work, the standard choices for these parameters are

$$\rho = 1, \quad \chi = 2, \quad \gamma = \frac{1}{2}, \quad and \quad \sigma = \frac{1}{2} \tag{4.11}$$

The algorithm then modifies this simplex repeatedly according to the following procedure:

1. Order: Each new iteration of the algorithm begins by labeling the vertices of the simplex

$$x_1, x_2, \ldots, x_{n+1} \tag{4.12}$$

such that

$$f(x_1) \leq f(x_2) \leq \ldots \leq f(x_{n+1}) \tag{4.13}$$

The vertex corresponding to the highest function value, x_{n+1}, is discarded and another point is added as the vertex. The choice of this other point depends on a number of rules that are explained below.

2. Reflect: First the reflected point x_r, is generated

$$x_r = \bar{x} + \rho(\bar{x} - x_{n+1}) = (1+\rho)\,\bar{x} - \rho\, x_{n+1} \tag{4.14}$$

$$\bar{x} = \sum_{i=0}^{n} \frac{x_i}{n} \tag{4.15}$$

Calculate the function value of the point $x_r, f(x_r)$. If $f(x_1) \leq f(x_r) < f(x_n)$, then add the point r as the new vertex to the simplex and terminate this iteration.

3. Expand: If $f(x_r) < f(x_1)$, calculate the expansion point x_e,

$$x_e = \bar{x} + \chi(x_r - \bar{x}) = \bar{x} + \rho\chi\left(\bar{x} - x_{n+1}\right) = (1+\rho\chi)\bar{x} - \rho\chi x_{n+1} \tag{4.16}$$

Calculate the function value of the point $x_e, f(x_e)$. If $f(x_e) < f(x_r)$, accept x_e as the new vertex and terminate the iteration. Otherwise, the point x_r is the new vertex.

4. Contract: If $f(x_r) \geq f(x_n)$, do a contraction either outside or inside based on whether x_r or x_{n+1} is better.

   a. Outside: If $f(x_n) \leq f(x_r) < f_{n+1}$, calculate the outside contraction point x_{co},

$$x_{co} = \bar{x} + \gamma(x_r - \bar{x}) = \bar{x} + \gamma\rho(\bar{x} - x_{n+1}) = (1+\rho\,\gamma)\bar{x} - \rho\gamma\, x_{n+1} \tag{4.17}$$

   If $f(x_{co}) \leq f(x_r)$, choose x_{co} as the new vertex and terminate this iteration, else perform a shrink operation.

   b. Inside: If $f(x_r) \geq f_{n+1}$, calculate the inside contraction point x_{ci},

$$x_{ci} = \bar{x} - \gamma(\bar{x} - x_{n+1}) = (1-\gamma)\bar{x} + \gamma x_{n+1} \quad (4.18)$$

If $f(x_{ci}) < f(x_{n+1})$, choose x_{ci} as the new vertex and terminate this iteration, else perform a shrink operation.

5. Shrink: This step shrinks the simplex around the vertex having the least function value i.e. x_1. This is done by replacing all the vertices with the equation below

$$x_i = x_1 + \sigma(x_i - x_1), \quad i = 2,3,..,n+1 \quad (4.19)$$

6. Check for Termination: Terminate the algorithm if any of the stopping criteria is satisfied. Otherwise, repeat the procedure from step 1.

The simplex search algorithm described above is illustrated on a 2-simplex in Figures 4.5 and 4.6. Both the nonlinear least squares algorithm and simplex search algorithms are quite commonly used. They are available in Simulink Response Optimization toolbox from Matlab. This toolbox is explained in the next section.

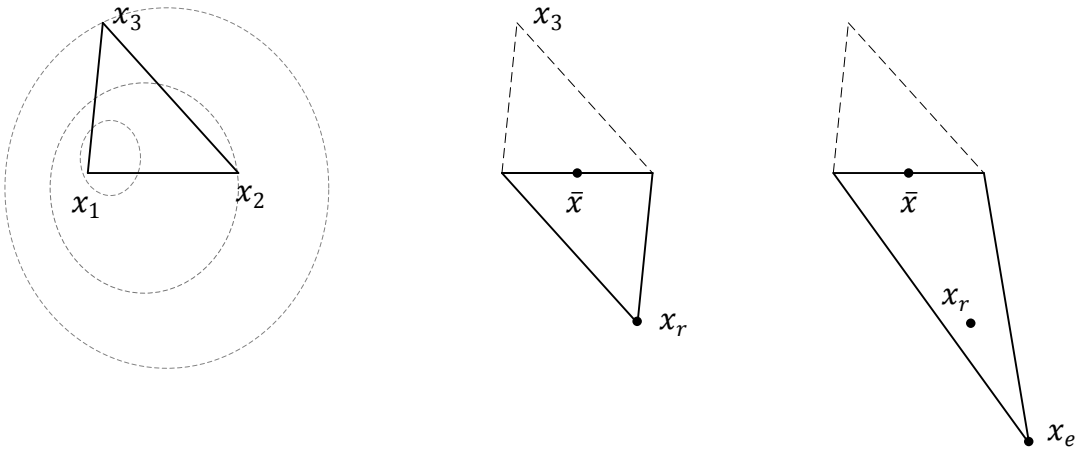

Fig. 4.5 Nelder Mead 2-Simplices with order, reflect and expand operations performed

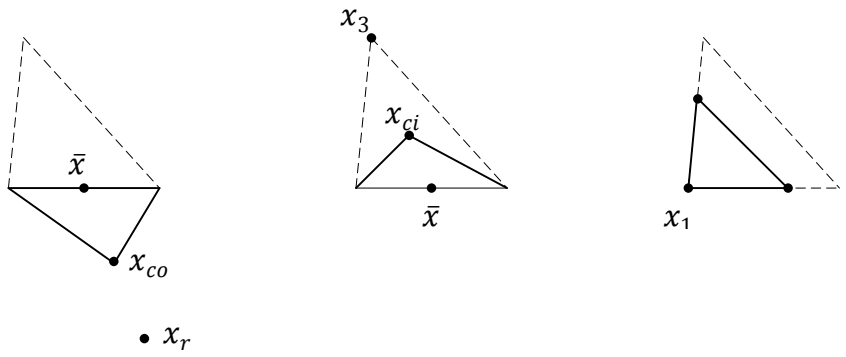

Fig. 4.6 Nelder Mead 2-Simplices with contract outside, contract inside and shrink operations performed

4.4 Simulink Response Optimization Toolbox

Simulink Response Optimization (SRO) toolbox is an optional toolbox available with Matlab 2008a [4]. It is called the Simulink Design Optimization toolbox in Matlab 2009a. SRO works in the Simulink environment. A user can improve mathematical models by estimating and tuning model parameters using numerical optimization techniques. In addition to parameter estimation users can tune controller gains so that the system meets design specifications. The design specifications like error limit between the model and the output can be set on a time scale. Also system design specifications like rise time, settling time etc. can be set by the user. All this specifications are set in the signal constraint block. Figure 4.7 shows a screenshot of the signal constraint block with signal constraints placed by the user.

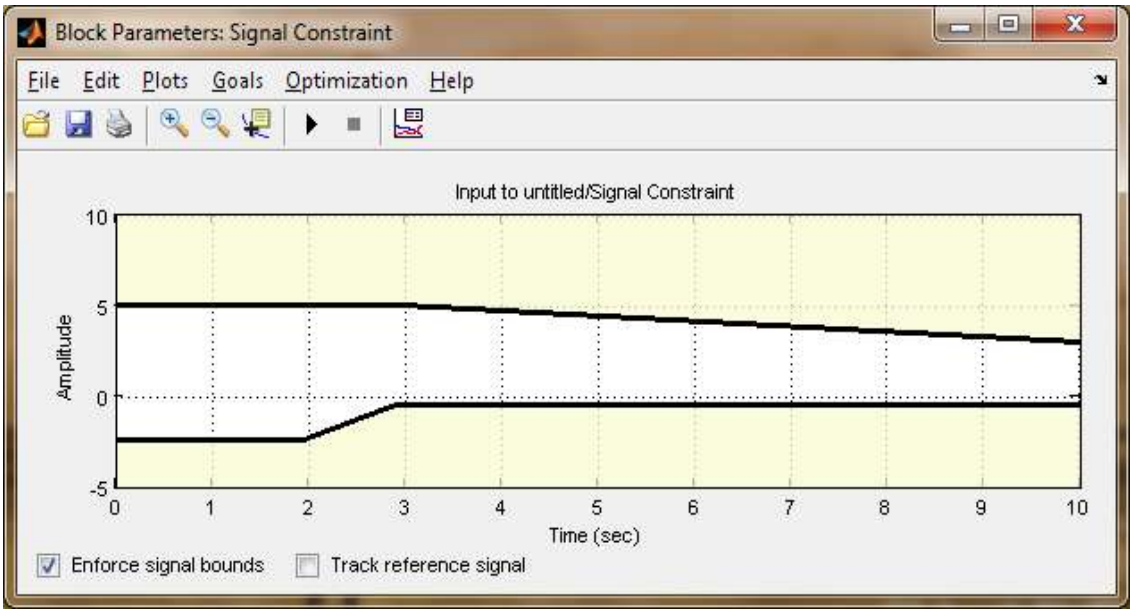

Fig. 4.7 Screenshot of the signal constraint block with signal constraints.

After choosing the signal constraints, one must choose the parameters that need to be tuned or estimated. Since this toolbox follows numerical search based algorithms for parameter estimation, one has to give initial values for the unknown parameters. The SRO toolbox gives the option of tuning the parameter by three numerical search methods, Nonlinear least squares, Simplex search and Pattern search algorithms. Users can choose any of these algorithms based on the requirement. Also once an algorithm is chosen the user can specify the tolerances associated with the parameters, constraints and the function. The function tolerance acts as a termination condition if the "Look for maximally feasible solution" box is checked else the numerical search stops when the system response is within the signal constraints. Figure 4.8 shows the layout of the different options available with the simplex search algorithm.

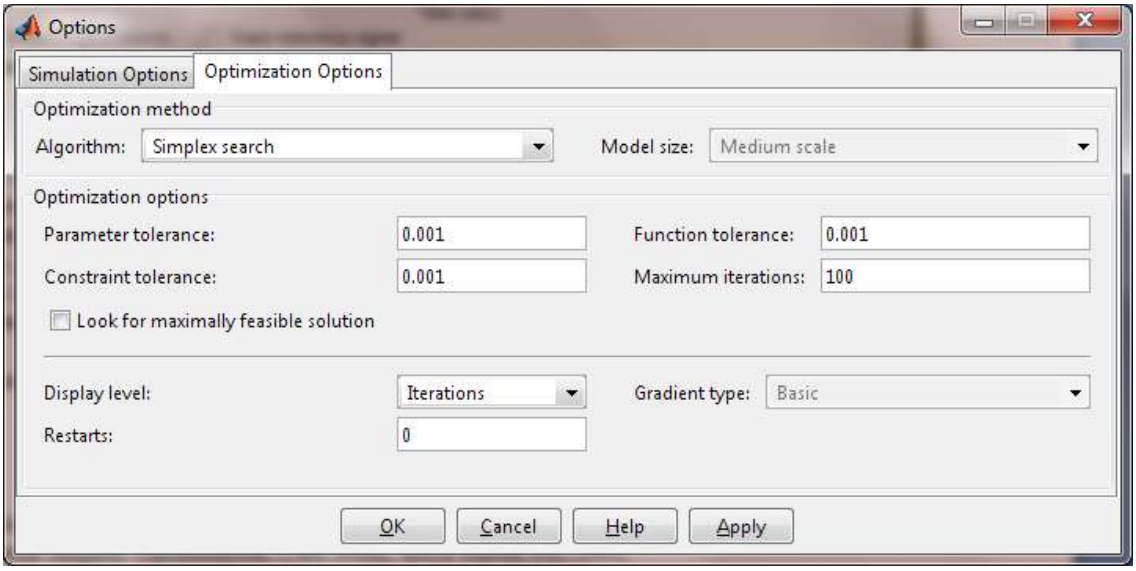

Fig. 4.8 The different options available with a numerical search algorithm

CHAPTER V

PARAMETER ESTIMATION PROCEDURE AND RESULTS

In this chapter the parameter estimation procedure that was used to estimate the parameters of the expansion valve and the compressor simultaneously is discussed. Firstly, the procedure to estimate the parameters of the valve and compressor given access to a mass flow meter will be seen followed by the method to estimate them without using the mass flow meter measurements.

In both the experimental set ups described in the third chapter, it was seen that the mass flow meter is placed right before the expansion valves and there is no mass flow meter next to their compressor. The reason for this being that the refrigerant is always in liquid phase only before the expansion device. It is economical to measure liquid flow than gaseous or multiphase fluid flow.

One can estimate the parameters of the expansion valve using even the transient components of a data set, but due to the constraint of not having a mass flow meter at the inlet to the compressor, its parameters can be estimated using only the steady state components of a data set. The estimation of the EEV and compressor parameters given the mass flow measurements can be performed by any regression technique. For this research the Least squares algorithm, explained in Chapter IV, was used. The results of parameter estimation using the mass flow meter information are provided in the Tables 5.1 and 5.2 on pp. 41 and 44 respectively. In case of the TEV, parameter estimation is

possible by sensing the temperature of the TEV bulb and the refrigerant temperature in the tube close to the point where the TEV bulb is installed.

In all the cases discussed so far the parameter estimation routine needs at least the presence of a single mass flow meter in the refrigerant loop. But there are a lot of commercial systems which don't have a mass flow meter in them due to the high cost of the sensor. For such systems it is possible to estimate the parameters of the expansion valve and compressor using the procedure discussed in this chapter.

5.1 Model Augmentation

The linearized continuous time evaporator model is augmented with the nonlinear expansion valve and compressor models. The resulting model's inputs are the pressure and temperature of the refrigerant at expansion valve inlet, temperature and mass flow rate of the secondary coolant over the evaporator coils, the EEV input in case an EEV is used, the compressor's operating frequency if it is known, and the initial estimates of the parameters. The output of the augmented model is the pressure and enthalpy of the refrigerant at the evaporator exit.

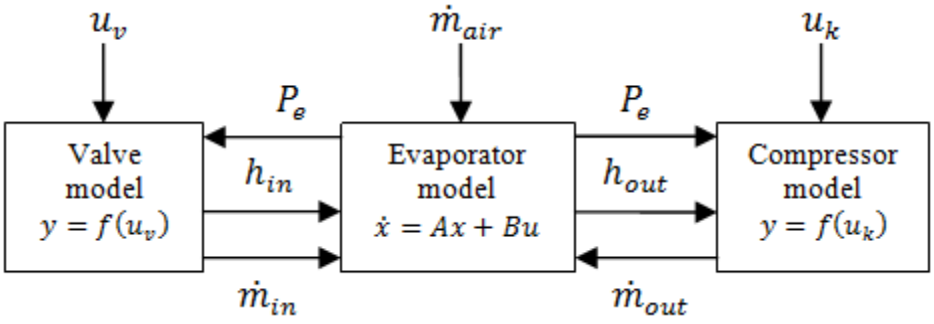

Fig. 5.1 Graphical representation of the augmented model

In case of an EEV, the system is excited by step inputs to the expansion valve. In case of a TEV, the system is excited by varying the flow rate of the secondary coolant over the evaporator coils. In both the cases, if a variable speed compressor is used, the compressor speed also needs to be changed to get the correct parameter values of the compressor model.

The output of the augmented model is compared with the experimental data and the error found. This error was minimized by using both the nonlinear least squares algorithm and the simplex search algorithm. The error in each output i.e. the pressure and the enthalpy are scaled so that equal weights are assigned for both the errors. This was necessary for the algorithm to return with the right estimates of the parameters. The error equation is given by

$$Error = \sum_{i=0}^{n} s_1\left(Pe_i - \widehat{Pe}_i\right)^2 + s_2\left(T_{ero\ i} - \hat{T}_{ero\ i}\right)^2 \quad (5.1)$$

In both the algorithms discussed here, initial values of the parameters need to be provided and it is important that these values are not way too far from the actual values. The initial estimates for the EEV, TEV and the compressor parameters used are given in Tables 5.1, 5.2 and 5.3.

5.2 Parameter Estimation of the EEV

As mentioned in Chapter 3, there are two independent experimental systems having an EEV as the expansion device. One is a custom built water chiller system and the other being a residential air conditioning system. The parameter estimation algorithm

was tried on both these systems. First the results of parameter estimation obtained on the residential air-conditioning unit are presented followed by the water chiller system.

5.2.1 EEV Parameter Estimation on the Residential Air Conditioner

The EEV opening is changed as seen in Figure 5.2. In Figure 5.3 it can be seen that the parameter estimation algorithm (simplex search) is able to find the parameters such that the predicted mass flow rate is exactly the same as the measured mass flow rate. Figures 5.4 and 5.5 show that the parameter estimation algorithm was successful in reducing the error as defined in Eq. (5.1).

Similar results were obtained with nonlinear least squares. The time taken for Simplex search and nonlinear least squares given the same initial estimate as mentioned in Table 5.1 is 360 and 700 seconds respectively. A comparison of both these methods with respect to error and speed is given in Table 5.1.

Table 5.1 EEV parameter estimation using different approaches for a dataset with 4200 samples. Linearized evaporator used.

Estimation method	EEV Parameters		Compressor Parameters		RMS error in mass flow rate at valve (grams/second)	Time taken (seconds)
	v_1	v_2	k_1	k_2		
Initial Parameters	-1.70	1.00	-2.46	1.00	–	–
Mass flow measurements	$-7.67 * 10^{-3}$	1.93	9.16	1.54	0.152	1
Simplex search	$-1.34 * 10^{-2}$	1.94	9.05	1.59	0.151	360
Nonlinear least squares	$-7.63 * 10^{-2}$	1.97	9.05	1.59	0.156	700

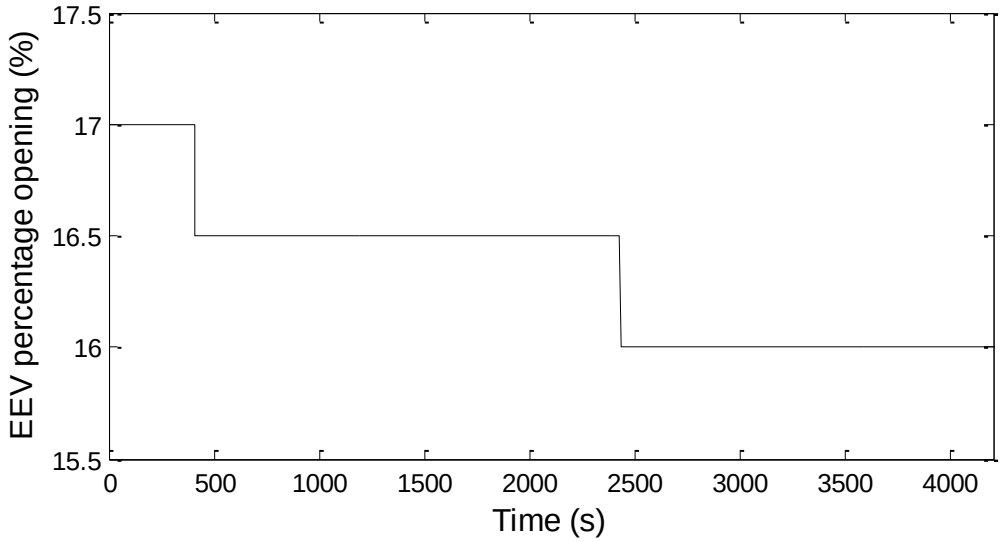

Fig. 5.2 EEV opening.

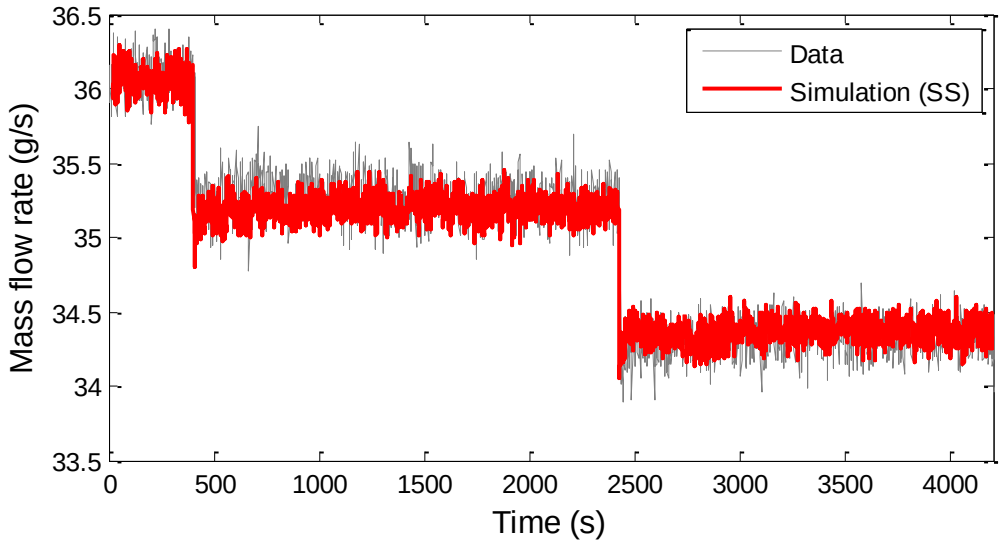

Fig. 5.3 Comparison of mass flow rate at the EEV inlet

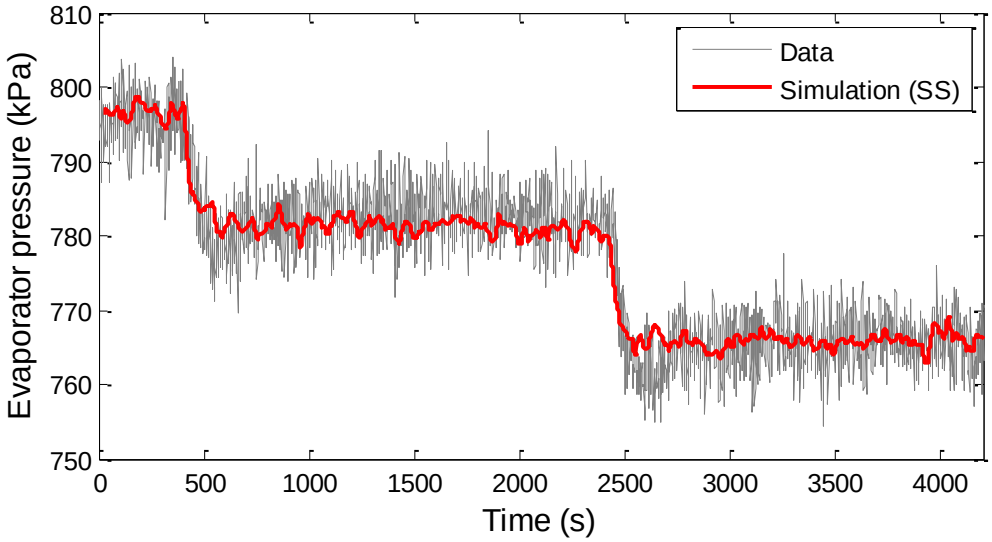

Fig. 5.4 Comparison of evaporator pressure

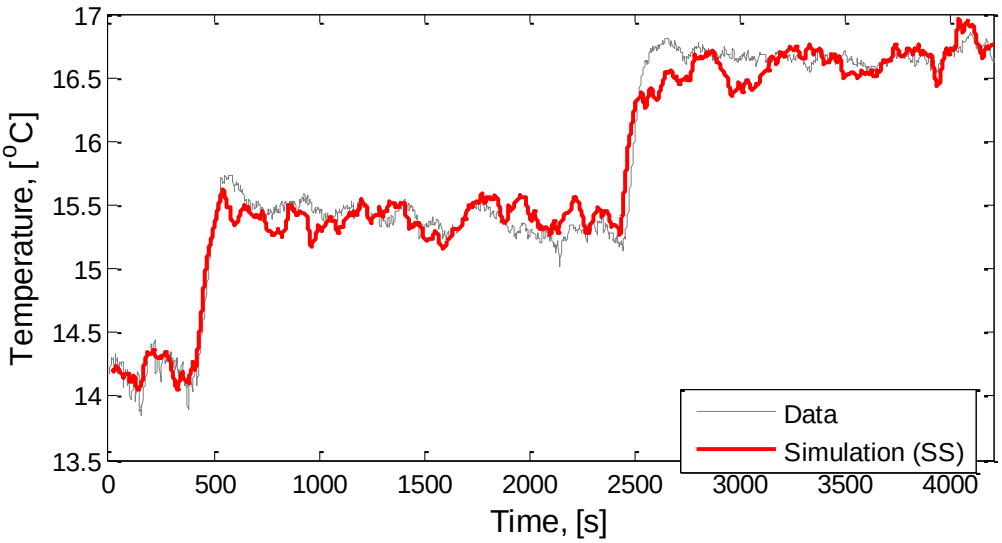

Fig. 5.5 Comparison of refrigerant temperature at evaporator exit

5.2.2 EEV Parameter Estimation on the Water Chiller System

The EEV position is changed as seen in Figure 5.6. Simplex search was used for this parameter estimation. The parameter estimates from this algorithm can be seen in Table 5.2. Using the estimated parameters the augmented model is simulated and the results can be seen in Figures 5.8 and 5.9. From these plots it is clear that the parameter estimation algorithm is able to estimate the parameters such that it is not only good enough for model simulation but is also accurately able to predict the mass flow rate of the refrigerant at the EEV as seen in Figure 5.7.

Table 5.2 EEV parameter estimation using different approaches for a dataset with 1500 samples. Linearized evaporator model used.

Estimation method	EEV Parameters		Compressor Parameters		RMS error in mass flow rate at valve (grams/second)	Time taken (seconds)
	v_1	v_2	k_1	k_2		
Initial Parameters	1.0	1.0	1.0	1.0	–	–
Mass flow measurements	-3.457	0.808	0.999	0.098	0.274	1
Simplex search	- 3.304	0.796	0.974	0.105	0.269	680
Nonlinear least squares	-3.414	0.803	0.976	0.101	0.277	780

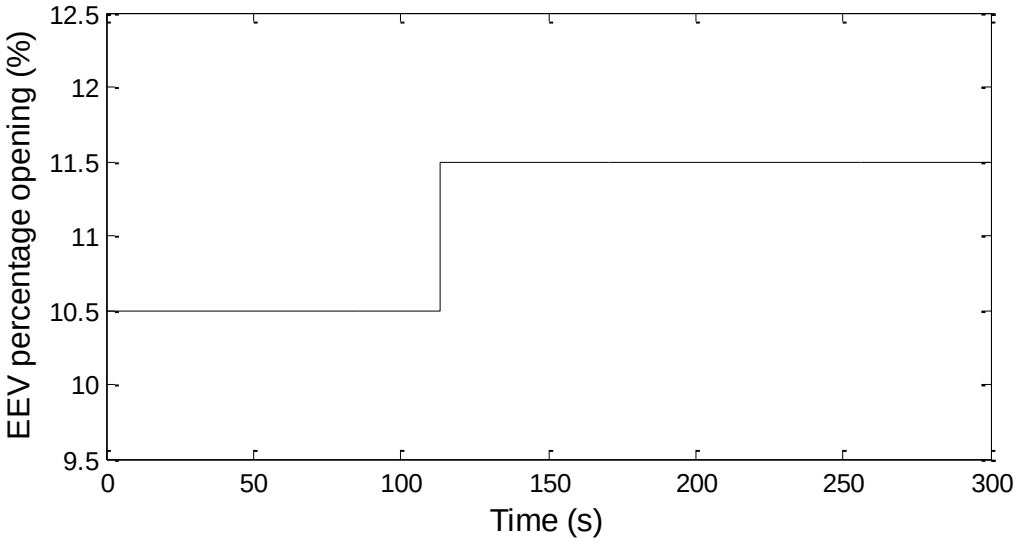

Fig. 5.6 EEV opening

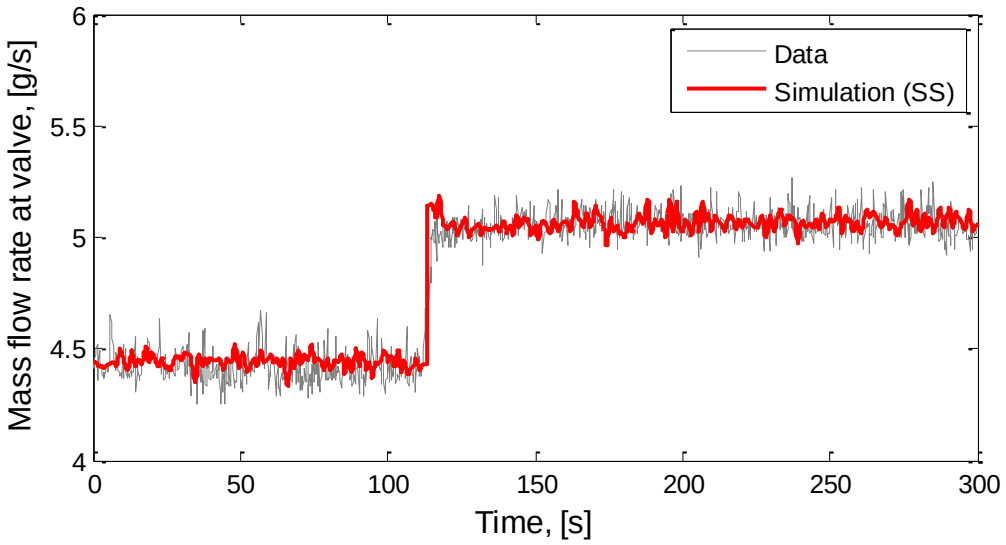

Fig. 5.7 Comparison of mass flow rate at the EEV inlet

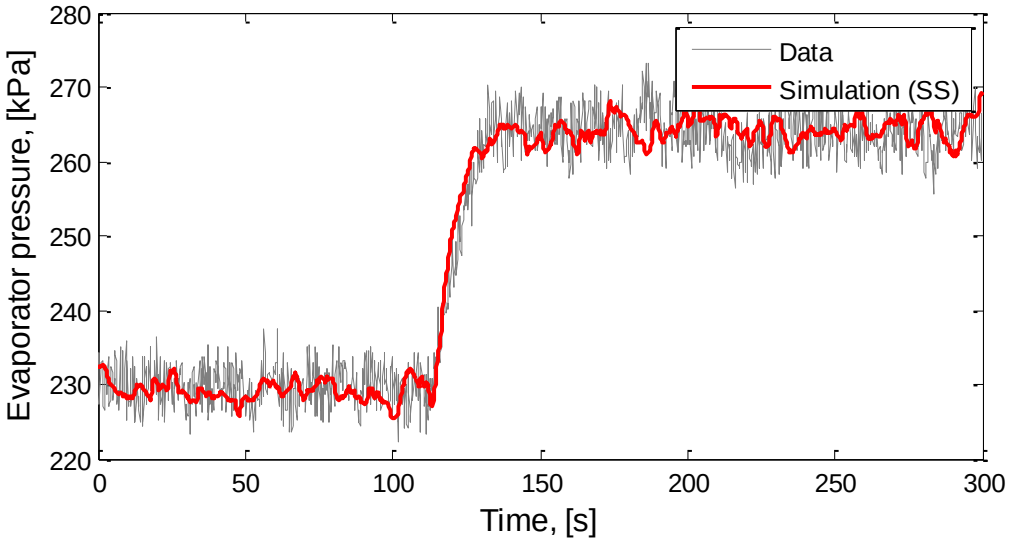

Fig. 5.8 Comparison of evaporator pressure

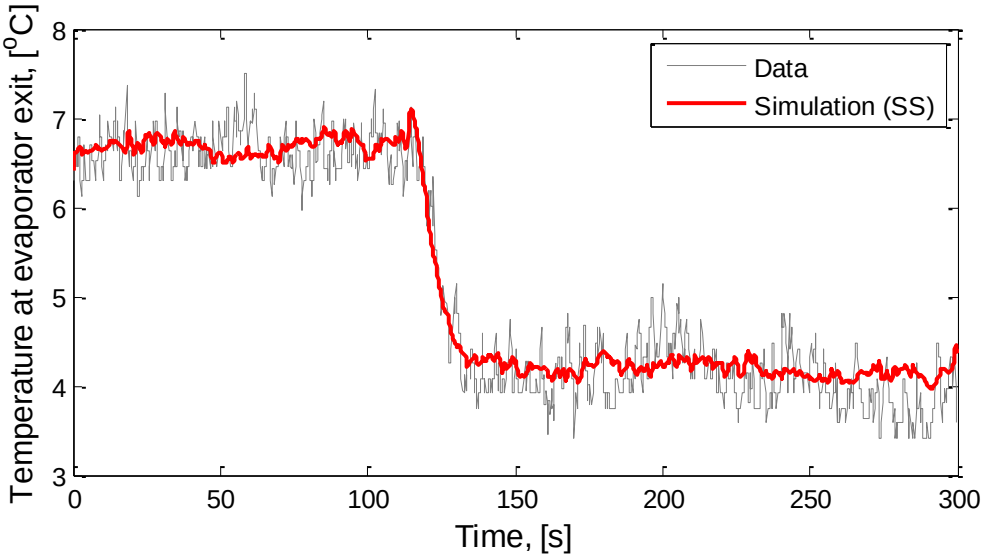

Fig. 5.9 Comparison of refrigerant temperature at evaporator exit

5.3 Parameter Estimation of the TEV

Eq. 2.5 and 2.11 is used to model the TEV. It is known that the area of opening of a valve is very small in the scale of millimeters. But in the TEV model the area is in m^2. This causes the parameters to have a very low value, in the order of 10^{-6}. So to scale the parameters the TEV model Eq. 2.11 was multiplied by 10^{-6}. The compressor speed during the test was 1500 RPM, i.e. 30 Revolutions per second. The internal volume of the compressor was not known. It is assumed to be 10 cm^3. Thus the compressor model is,

$$\dot{m}_k = 30 * 10 * 10^{-6}(k_1 - k_2(P_c/P_e))\rho_k \tag{5.2}$$

The scaled TEV model, compressor model given in Eq. 5.2 and the linearized continuous time evaporator model are augmented for this problem. The water flow rate over the evaporator is varied as shown in Figure 5.10. The initial values of the parameters are given in Table 5.3. With the estimated parameters the model is simulated and is compared with experimental data in Figures 5.11 – 5.13. While estimating the parameters of the EEV, it was seen that the Simplex search algorithm was a faster algorithm but for the TEV case, which is a more complex problem, it took a longer time. The reason for this is that the algorithm settles at a local minima (the Simplex shrinks to a point) and the optimization routine needed to be restarted. For this case the nonlinear least squares definitely provides a better estimate which can be seen by the difference in RMS error or by comparing the Figures 5.11 to 5.13. From the close match seen between the experimental data and the model outputs it is safe to say that the parameter estimation approach has worked well in this case.

Table 5.3 TEV parameter estimation using different approaches for a dataset with 2000 samples. Linearized evaporator model used.

Estimation method	TEV Parameters			Compressor Parameters		RMS error in mass flow rate at valve (grams/second)	Time taken (seconds)
	v_1	v_2	$\tau\ (s)$	k_1	k_2		
Initial Parameters	1.00	1.00	10.0	1.00	1.00	–	–
Simplex search	5.60	3.01	46.9	0.94	0.20	0.6766	1200
Nonlinear least squares	5.31	3.12	40.9	0.94	0.20	0.5365	610

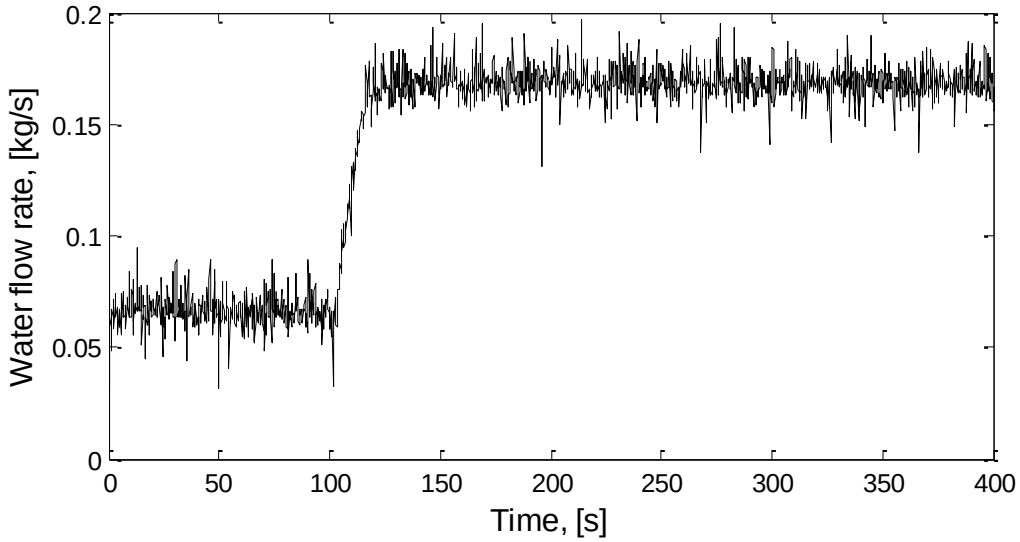

Fig. 5.10 Water flow rate.

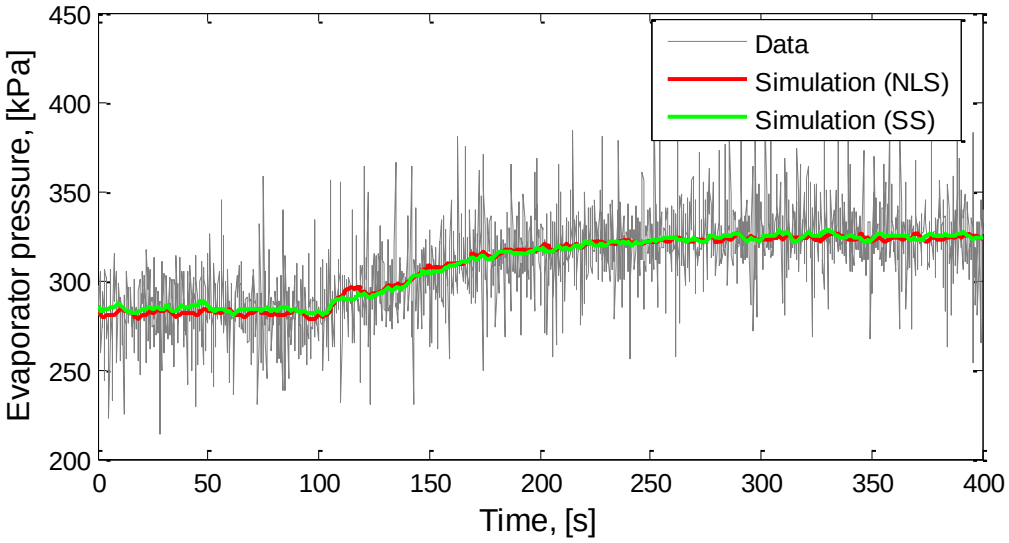

Fig. 5.11 Comparison of evaporator pressure

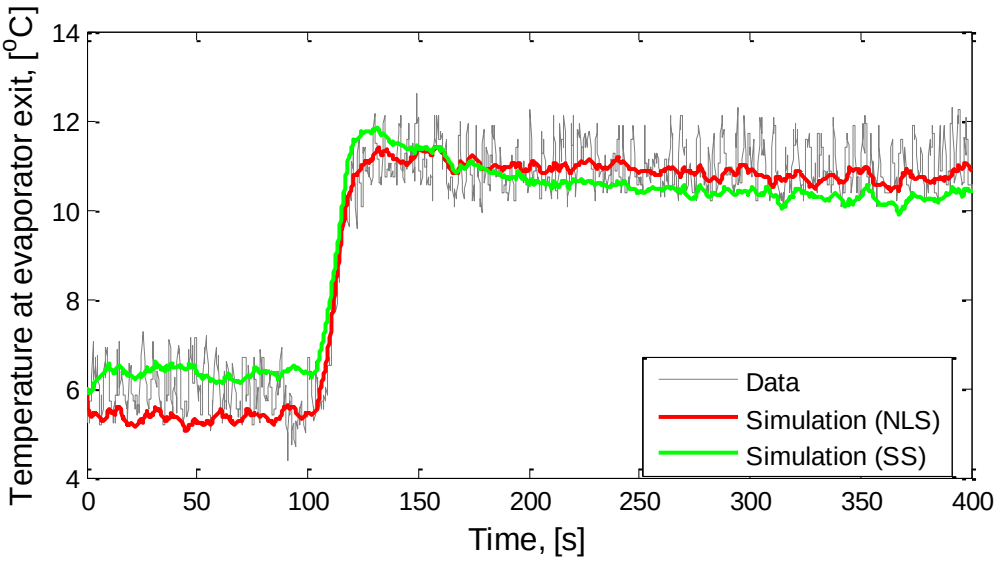

Fig. 5.12 Comparison of refrigerant temperature at evaporator exit

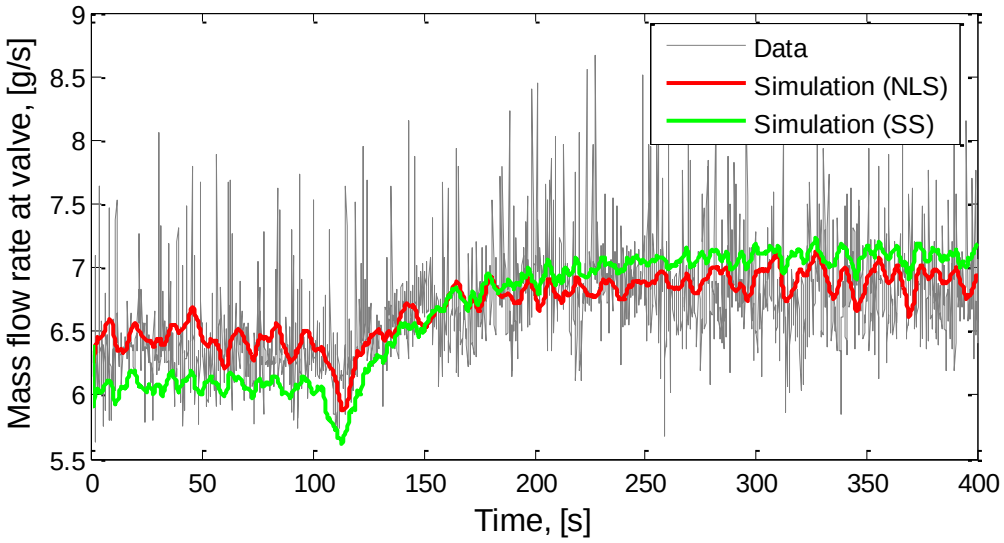

Fig. 5.13 Comparison of mass flow rate at the TEV inlet

The above experimental results indicate that the parameter estimation method is successfully able to identify the parameters when the initial estimates are far from the final value by an order of magnitude and is robust enough to overcome the problems of measurement noise, unmodeled dynamics. Also the time consumed for parameter estimation is low. The results indicate that the nonlinear least squares algorithm is better suited for this estimation problem.

5.4 Parameter Spread

Parameter spread is studied to find the suitability of the valve and compressor parameters found in a particular test to be used again in a subsequent test with similar operating conditions. The parameter spread is found in this section by comparing the parameters estimated by performing similar valve step changes at different instances of time. Figure 5.14 shows the valve positions as a function of time. In case of a TEV, the

external flow rate of the coolant is changed as shown in Figure 5.15. The parameter spread is computed in Table 5.4.

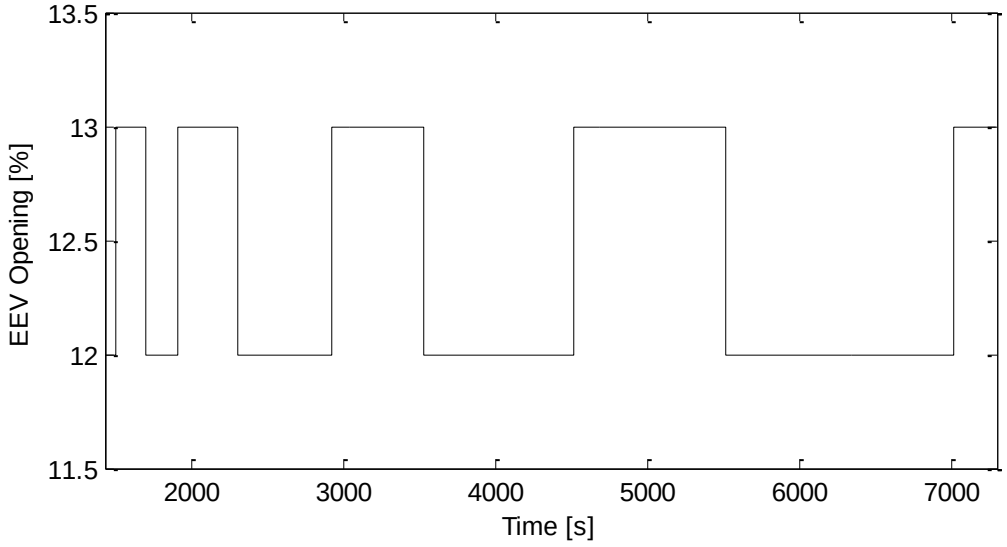

Fig. 5.14 EEV opening as a function of time

Table 5.4 Valve and compressor parameters at different instances of time

S.No	EEV parameters		Compressor parameters		TEV Parameters	
	v_1	v_2	k_1	k_2	v_1	v_2
1	-6.0927	1.0240	1.3620	0.0580	1.4102	1.5278
2	-5.3748	0.9344	1.2450	0.0579	1.0504	1.6372
3	-5.1241	0.9153	1.3181	0.0324	1.2206	1.5624
4	-5.2466	0.9260	1.2594	0.0497	1.5443	1.4722
Parameter Spread	15.90 %	10.62 %	8.59 %	44.14 %	31.98 %	10.08%

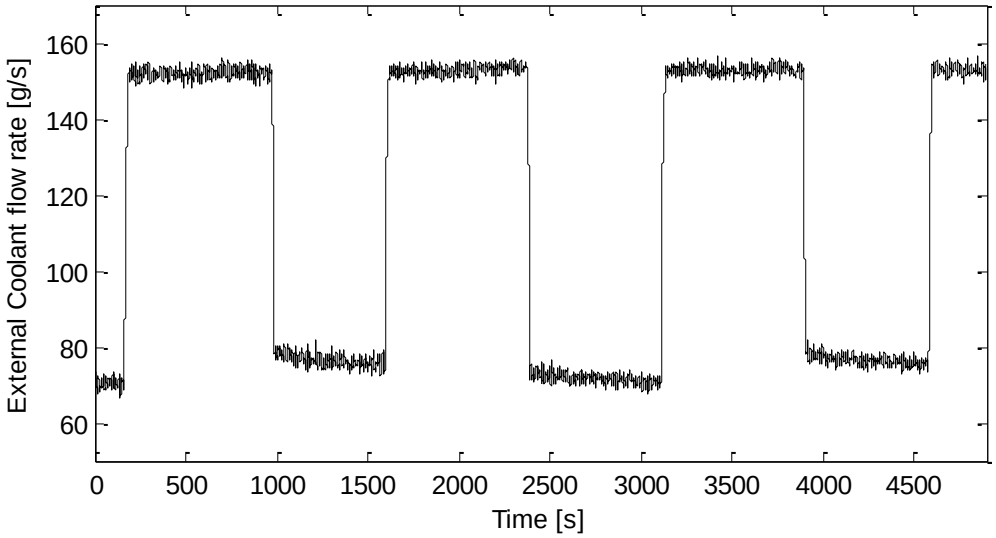

Fig. 5.15 Water flow rate over the evaporator as a function of time

5.5 Parameter Sensitivity

Parameter sensitivity of the various parameters of the EEV, TEV and the compressor are analyzed in this section. Each component's parameter values is increased by 10% - 50%, (depending on the parameter spread) while keeping the values of the other component's parameters equal to the values estimated using the flow rate data. After the parameter value has changed, the augmented model is simulated. First an augmented model with an EEV and a compressor is simulated, followed by the model with a TEV and a compressor. The simulated evaporator pressure, temperature of the refrigerant at evaporator outlet, and the mass flow rate of the refrigerant is compared with the simulation obtained using the actual values of the parameters. These comparisons are given in Figures 5.16-5.27. From these plots, one can conclude that the parameters estimated for components in one test can be reused to model a different test

with similar operating conditions. This is a main requirement considering the fact that the parameter estimation algorithm currently used is an offline technique.

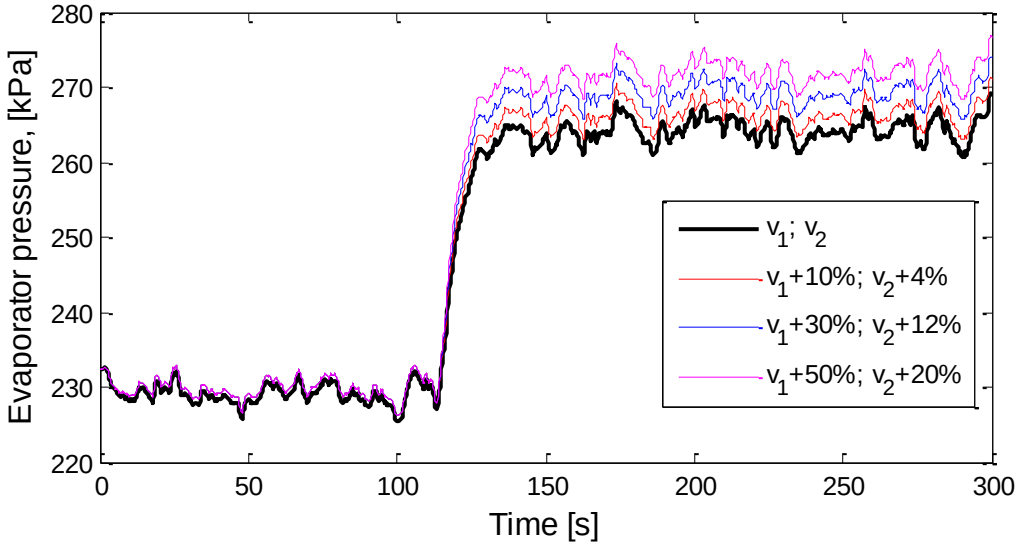

Fig. 5.16 Simulated evaporator pressures as the EEV parameters are changed

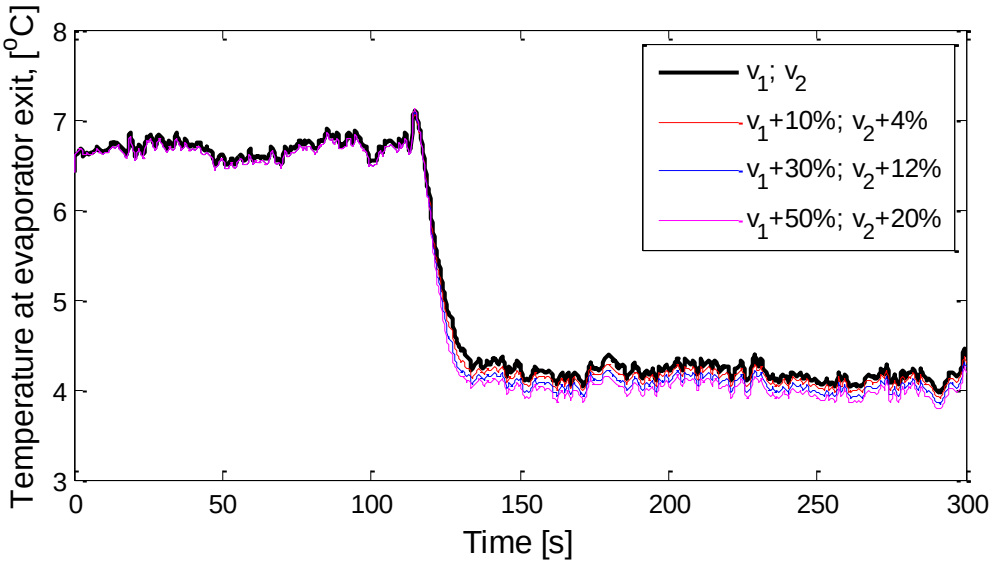

Fig. 5.17 Simulated temperatures of the refrigerant at evaporator exit as the EEV parameters are changed

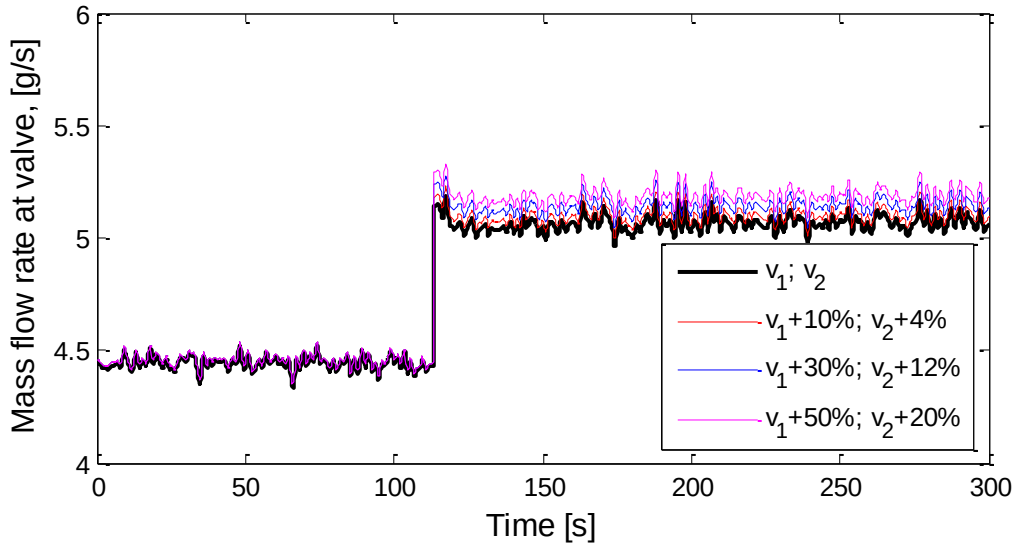

Fig. 5.18 Simulated mass flow rates at the valve inlet as the EEV parameters are changed

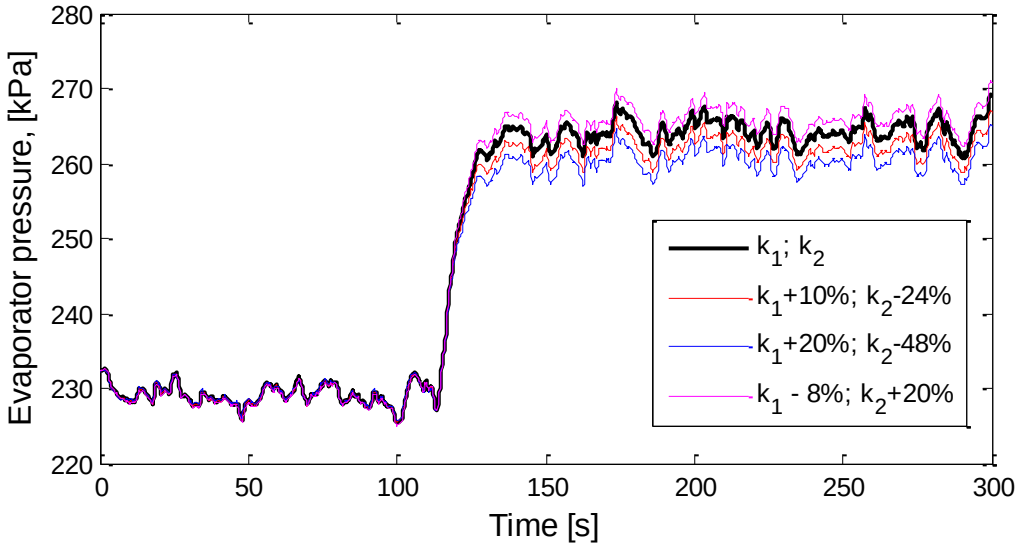

Fig. 5.19 Simulated evaporator pressures as the compressor parameters are changed

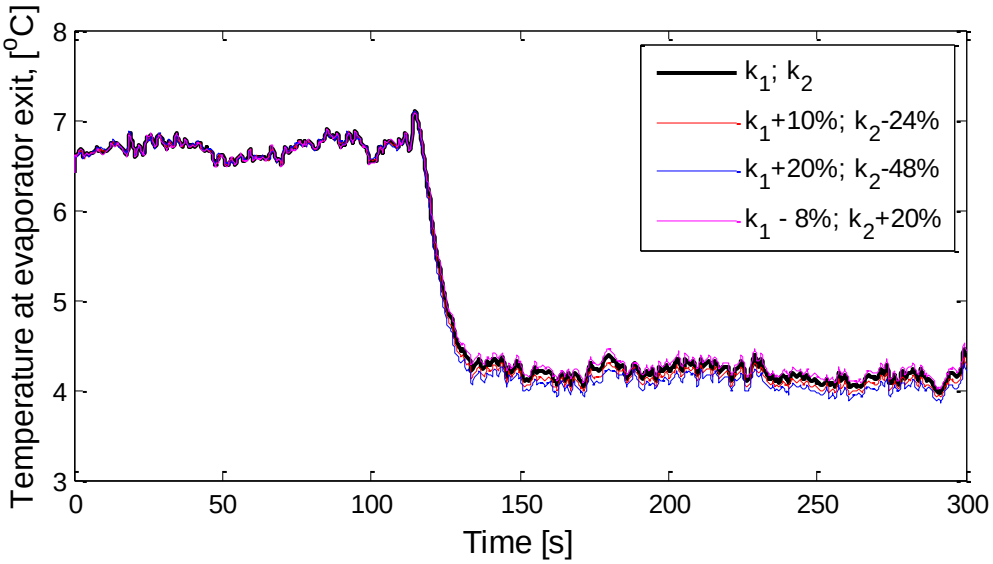

Fig. 5.20 Simulated temperatures of the refrigerant at evaporator exit as the compressor parameters are changed

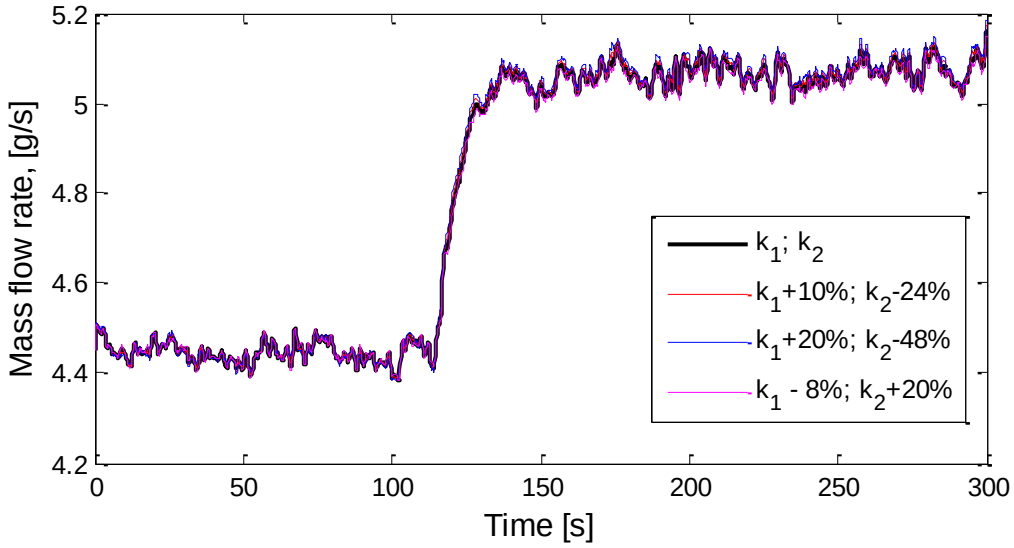

Fig. 5.21 Simulated mass flow rates of the refrigerant at the valve inlet as the compressor parameters are changed

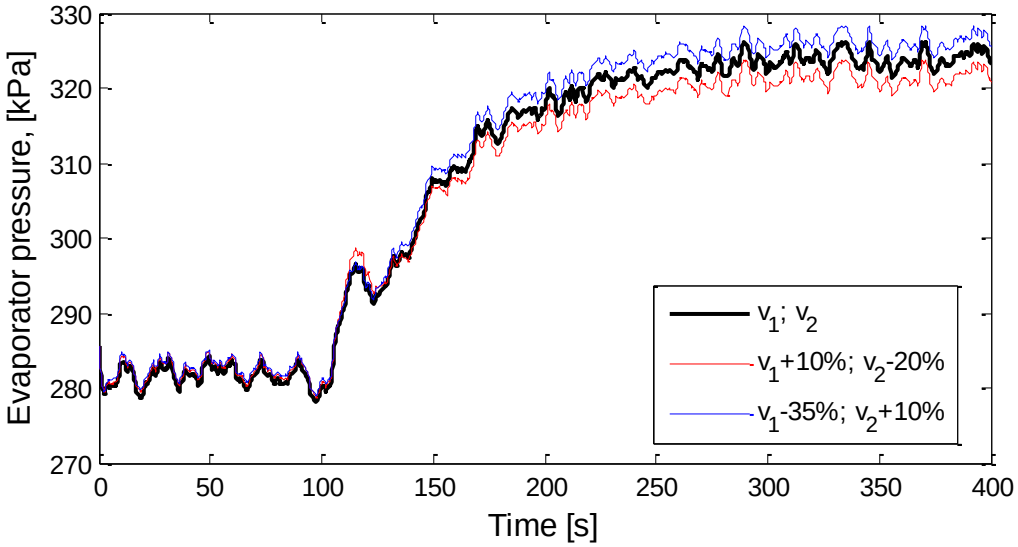

Fig. 5.22 Simulated evaporator pressures as the TEV parameters are changed

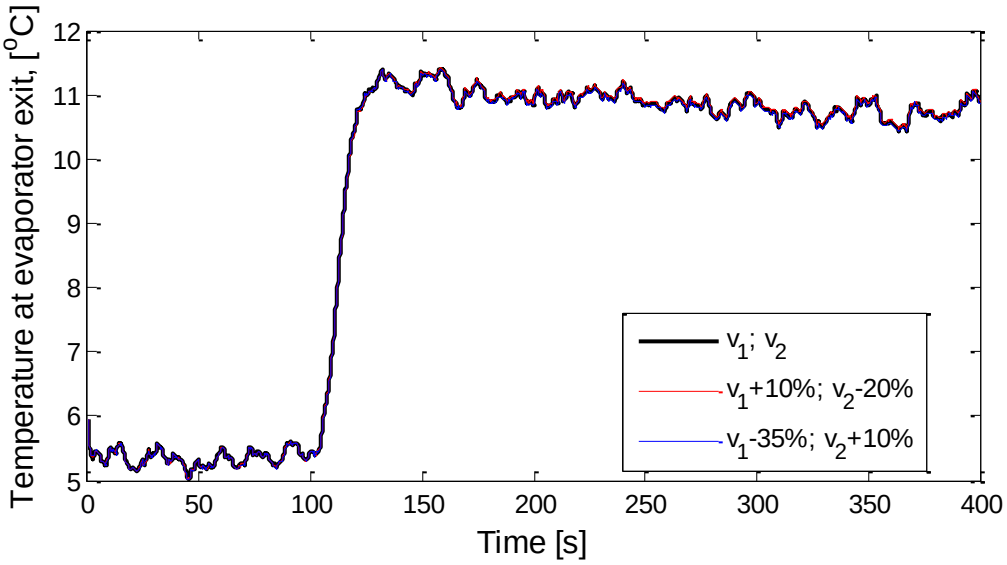

Fig. 5.23 Simulated temperatures of the refrigerant at evaporator exit as the TEV parameters are changed

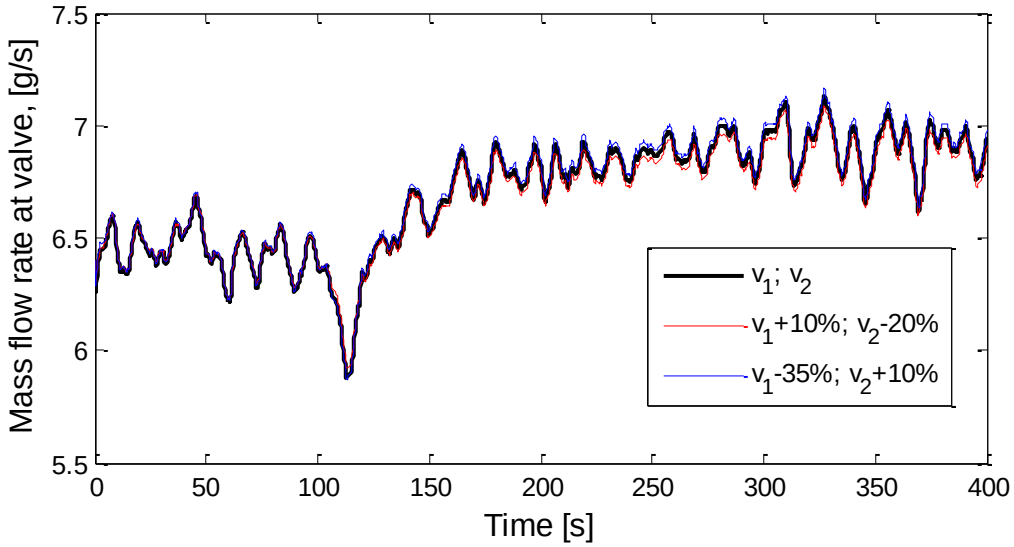

Fig. 5.24 Simulated mass flow rates of the refrigerant at the valve inlet as the TEV parameters are changed

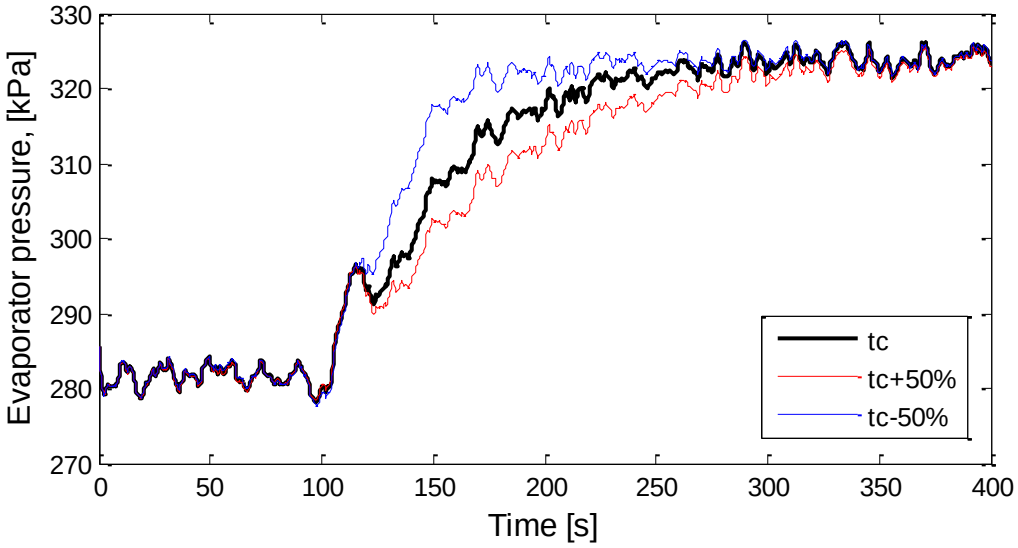

Fig. 5.25 Simulated evaporator pressures as the TEV parameter, t_c, is changed

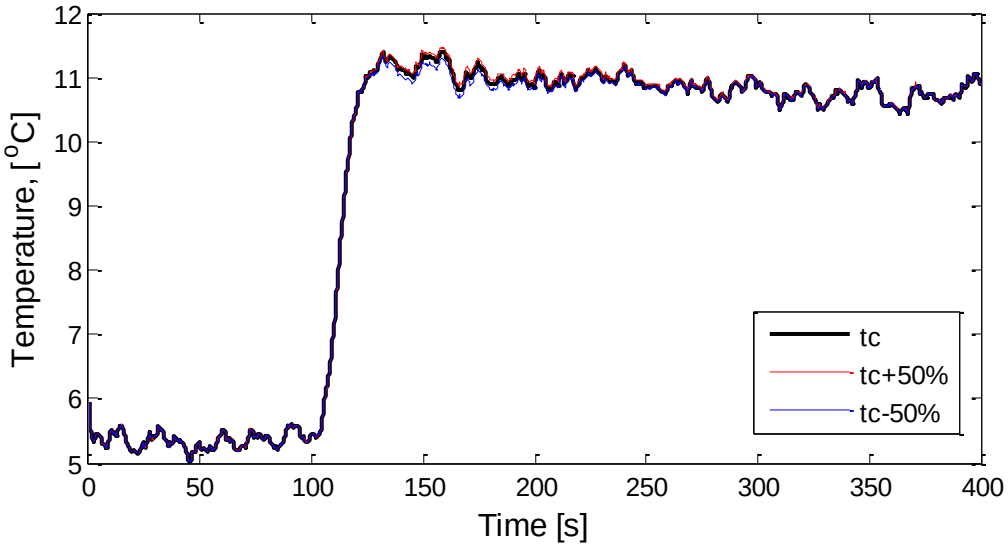

Fig. 5.26 Simulated temperatures of the refrigerant at evaporator exit as the TEV parameter, t_c, is changed

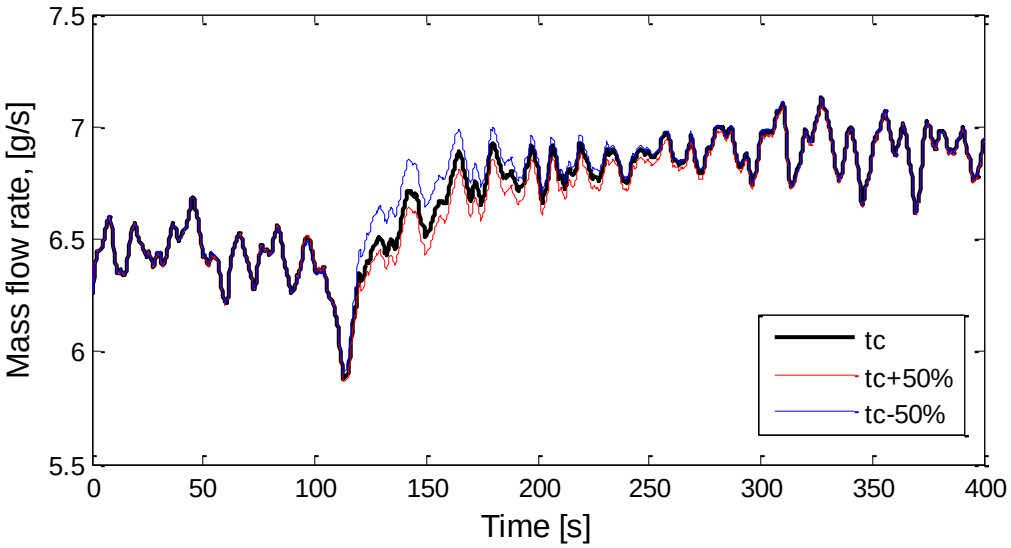

Fig. 5.27 Simulated mass flow rates of the refrigerant at the valve inlet as the TEV parameter, t_c, is changed

5.6 TEV Model Validation

An extensive review of the relevant literature revealed just one experimental validation of the TEV [9]. However, this lone case had limitations. Subsequently, one of the important aspects of this thesis was to develop a gray box model for the TEV and validate this model experimentally. Section 5.3 on parameter estimation of the TEV clearly shows that the TEV model is working well for those operating conditions. But in the water chiller system, there was almost no valve hunting and it was difficult to predict whether the TEV model would work in case there were any valve hunting. For this reason, the TEV model was validated on two other systems. One had an internally equalized TEV, similar to the one used in the water chiller system, installed on an air cooler system in the Air-Conditioning and Refrigeration Center at the University of Illinois at Urbana Champagne [19]. Another experimental set up was the residential air-conditioning unit mentioned in chapter III. This set up used an externally equalized TEV. The difference between an internally equalized and an externally equalized TEV is that in case of the former the refrigerant pressure at the inlet of the evaporator acts on the valve diaphragm and regulates the TEV opening. In case of the latter, the refrigerant pressure at the exit of the evaporator is used to regulate the diaphragm. Externally equalized TEVs are generally used in cases where there is a significant drop in the refrigerant pressure across the evaporator.

The air cooler system is similar to the water chiller system mentioned in Chapter III, with the significant difference being that the external coolant used is not water but air. In this system a variable speed compressor is used. To excite the system, the

compressor speeds are stepped as seen in Figure 5.28. Figure 5.29 shows the comparison of the simulated and experimental mass flow rates of the refrigerant at the TEV inlet. It can clearly be seen that the model is able to capture the valve hunting phenomenon.

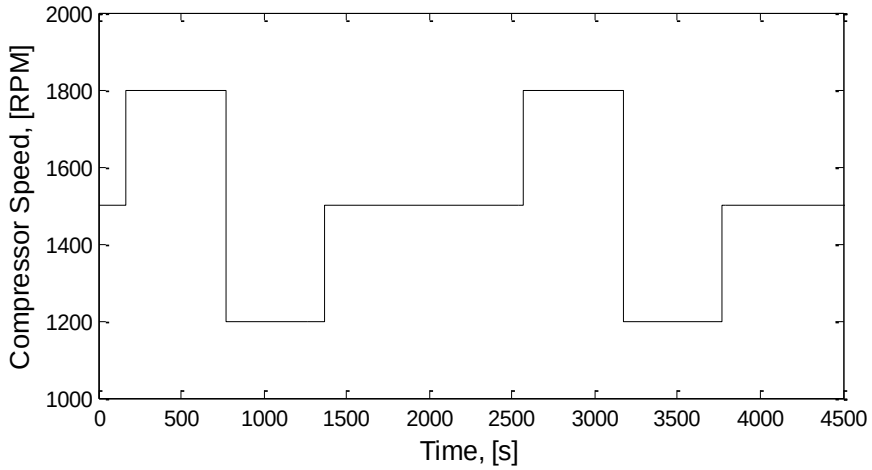

Fig. 5.28 Compressor speed changed to excite the system

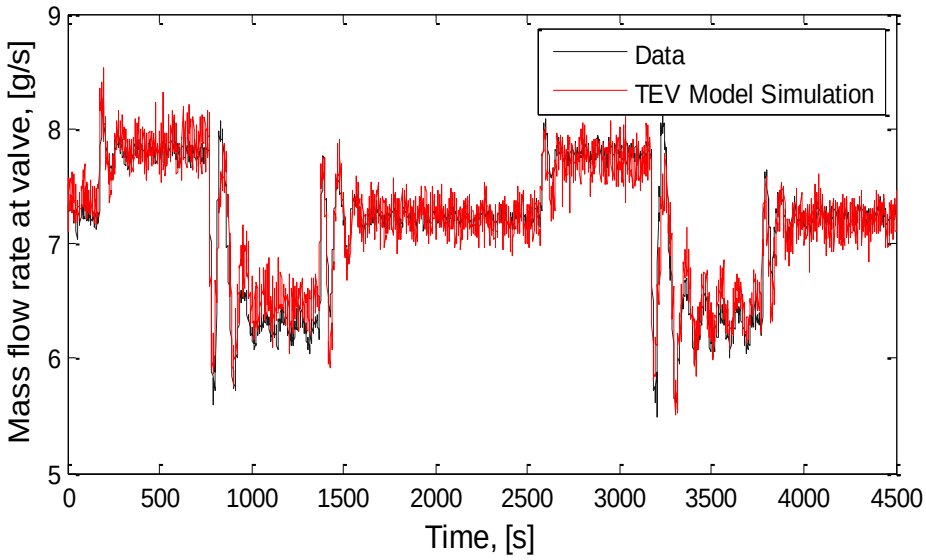

Fig. 5.29 Comparison of simulated and measured mass flow rates at TEV inlet

In the case of residential air conditioner system which has a constant speed compressor, the system was excited by varying the mass flow rate of the air over the evaporator coils. This was achieved by varying the evaporator fan speed. Figure 5.30 shows the change in fan speed voltage. Figure 5.31 shows the comparison of the simulated and experimental mass flow rates of the refrigerant at the TEV inlet. It can be seen that the TEV model is capturing the valve hunting phenomenon, but, one of the transient behaviors induced while changing the evaporator coolant flow rate is not being captured in the case of an externally equalized TEV. The reason for this behavior is under investigation and will be part of future work.

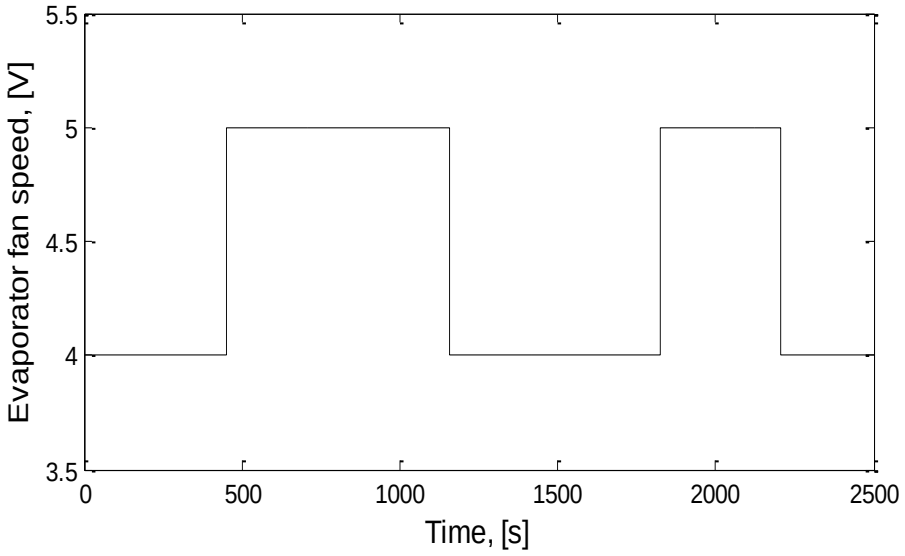

Fig. 5.30 Evaporator fan speed changed to excite the system

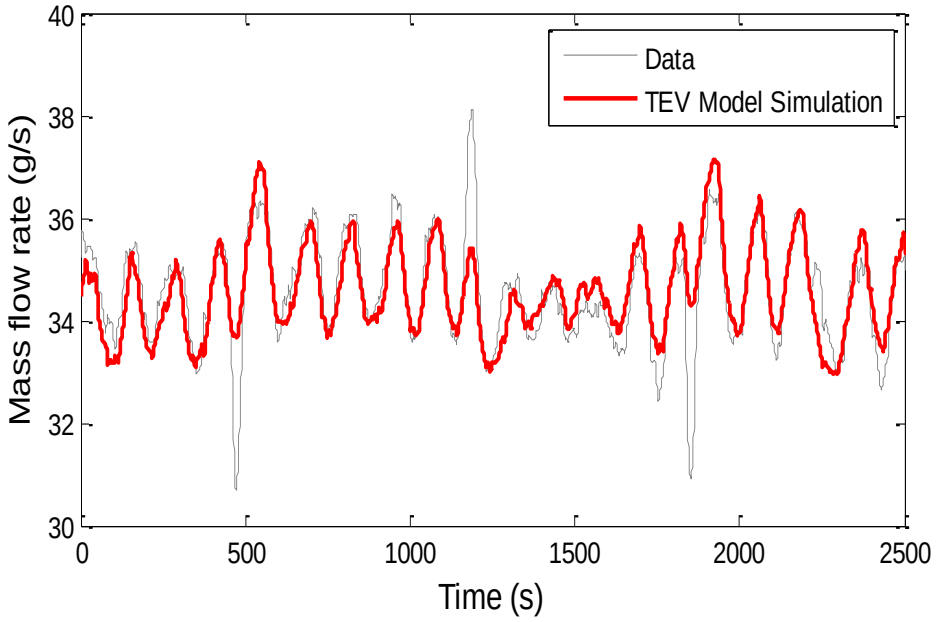

Fig. 5.31 Comparison of simulated and measured mass flow rates at TEV inlet

CHAPTER VI

CONCLUSION

This research makes several contributions to the field of AC&R modeling. A mathematical model of the Thermostatic Expansion valve has been provided and it has been validated with data. Prior work in this area had the limitation of the simulated data not agreeing well with the experimental data [9]. The present study, however, has mitigated that limitation.

A novel approach to estimate the empirical parameters of a dynamic air-conditioning model has been provided. Easy to use models have been presented for the EEV, TEV, evaporator and the compressor (both fixed speed and variable speed type) used in AC&R systems. The estimation problem was approached using Simplex search and nonlinear least squares algorithm. The nonlinear least squares algorithm proved to be more robust and also less time consuming for complex models. Parameter spread and sensitivity analysis performed show that the parameters estimated in a test can be used for another test with similar operating conditions, which is an important factor considering the offline estimation procedure.

The technique proposed here can be used with other types of grey box identification problems that are difficult to solve using the analytical identification methods, such as the least squares approach or the maximum likelihood method.

On the AC&R front there are a lot of applications for this work. Knowing the valve and compressor parameters, one can get accurate mathematical models which can

be used for control applications and fault detection purposes. Another important application is the development of virtual mass flow sensors.

In the present work, both the temperature and pressure sensors are being used to estimate the unknown parameters. Future research might consider the effectiveness of the estimation procedure with the use of only temperature measurements. This is desired due to the fact that thermocouples are much cheaper compared to pressure sensors and are also easy to operate. Another aspect that needs to be looked at is the development of an online estimation technique. This will be useful to continuously monitor HVAC systems.

REFERENCES

[1] Energy Information Administration, May, 2009, International Energy Outlook 2009 [Online]. Available: http://www.eia.doe.gov/oiaf/ieo/world.html

[2] Anonymous, 2006 Annual Energy Review 2005. DOE/EIA- 0384(2005). http://www.eia.doe.gov/emeu/aer/consump.html

[3] X-D He, S. Liu, and H. H. Asada, "Modeling of vapor compression cycles for multivariable feedback control of HVAC systems," *ASME Journal of Dynamic Systems, Measurement and Control*, vol. 119, pp. 183-191, 1997.

[4] Simulink Response Optimization User's Guide, The Math Works, Inc., Natick, MA, 2004.

[5] K. A. James and R. W. James, "Transient analysis of thermostatic expansion valve for refrigeration system evaporators using mathematical models," *Transacations of the Institute of Measurement Control*, vol. 9, pp. 198-205, 1987.

[6] M. R. O. Hargreaves and R. W. James, "A model of a marine water chilling plant for microprocessor control development," in *Proceedings of the Institute of Refrigeration*, London, 1979-80, vol. 76, pp. 28-30.

[7] P. M. T. Broersen, "Control with a thermostatic expansion valve", *International Journal of Refrigeration*, vol. 5, pp. 209-212, 1982.

[8] P. M. T. Broersen and M. F. G. Van der Jagt, "Hunting of evaporators controlled by a thermostatic expansion valve," *ASME Jounal of Dynamic Systems, Measurement and Control*, vol. 102, pp. 130-135, 1980.

[9] P. Mithraratne and N. E. Wijeysundera, "An experimental and numerical study of hunting in thermostatic expansion valve controlled evaporators," *International Journal of Refrigeration*, vol. 25, pp. 992-998, 2002.

[10] R. W. James and S. A. Marshall, "Dynamic analysis of a refrigeration system," in *Proceedings of the Institute of Refrigeration*, U.K., 1974, vol. 70, pp. 13-24.

[11] G. A. Ibrahim, "Theoretical investigation into instability of a refrigeration system with an evaporator controlled by a thermostatic expansion valve," *Canadian Journal of Chemical Engineering*, vol. 76, pp. 722-727, 1998.

[12] P. M. T. Broersen and J. ten-Napel, "Identification of a Thermostatic Expansion Valve," *Preprint IFAC Symposium on Identification and System Parameter Estimation*, Washington, DC, 1982, pp. 415-420.

[13] M. Dhar and W. Soedel, "Transient analysis of a vapor compression refrigeration system," in *Proceedings of the 15th International Congress of Refrigeration,* Venice, Italy, 1979, pp. 1035-1067.

[14] J. Chi and D. Didion, "A simulation of the transient performance of a heat pump," *International Journal of Refrigeration*, vol. 5, No. 3, pp. 176-184, 1982.

[15] M. Kapa and C. H. Wolgemuth, "A dynamic model of a condenser in a closed Rankine cycle power plant," in *Proceedings of the American Control Conference*, San Diego, CA, 1984, pp. 79-84.

[16] S. M. Sami, T. N. Duong, Y. Mercadier, and N. Galanis, "Prediction of the transient response of heat pumps," *ASHRAE Transactions*, vol. 93, Part 2, pp. 471-489, 1987.

[17] J. W. MacArthur and E. W. Grald, "Unsteady compressible two-phase flow model for predicting cyclic heat pump performance and a comparison with experimental data," *International Journal of Refrigeration,* vol. 12, pp. 29-41, 1989.

[18] G. L. Wedekind, B. L. Bhatt, and B. T. Beck, "A system mean void fraction model for predicting various transient phenomena associated with two-phase evaporating and condensing flows," *International Journal of Multiphase Flow,* vol. 4, pp. 97-114, 1978.

[19] B. P. Rasmussen, "Dynamic modeling and advanced control of air-conditioning and refrigeration systems," Ph.D. dissertation, Department of Mechanical Engineering, University of Illinois, Urbana-Champaign, IL, 2005.

[20] T. Pfafferott and G. Schmitz, "Numeric simulation of an integrated CO_2 cooling system," in *Proceedings of the Modelica 2000 Workshop*, Lund, Sweden, 2000, pp. 89-92.

[21] P. Mithraratne, N. E. Wijeysundera, and T. Y. Bong, "Dynamic simulation of a thermostatically controlled counter-flow evaporator," *International Journal of Refrigeration,* vol. 23, pp 174-189, 2000.

[22] S. Bendapudi, J. E. Braun, and E. A. Groll, "A comparison of moving-boundary and finite-volume formulations for transients in centrifugal chillers," *International Journal of Refrigeration*, vol. 31, pp. 1437-52, 2008.

[23] S. Bendapudi, "Development and evaluation of modeling approaches for transients in centrifugal chillers," Ph.D. dissertation, Department of Mechanical Engineering, Purdue University, IN, 2004.

[24] D. D. Wile, “The measurement of expansion valve capacity,” *Refrigeration Engineering*, vol. 8, pp.1–8, 1935.

[25] X. Zhifang, S. Lin, and O. Hongfei, “Refrigerant flow characteristics of electronic expansion valve based on thermodynamic analysis and experiment,” *Applied Thermal Engineering*, vol. 28, pp. 238–243, 2008.

[26] M. J. Lenger, A. M. Jacobi, and P. S. Hrnjak, "Superheat stability of an evaporator and thermostatic expansion valve," ACRC, University of Illinois, Urbana-Champaign, IN, TR - 138, 1998.

[27] A. Gupta, “Reduced order modeling of heat exchangers using high order finite control volume models,” TFCL, Texas A&M University, College Station, TX, A record of study, 2008.

[28] S. M. Zivi, “Estimation of steady state stream void fraction by means of the principle of minimum entropy production,” *ASME Journal of Heat Transfer*, vol. 86, pp. 247 - 252, 1964.

[29] J. P. Wattelet, J. C. Chato, B. R. Christoffersen, G. A. Gaibel, M. Ponchner, et al**.,** “Heat transfer flow regimes of refrigerants in a horizontal- tube Evaporator,” ACRC, University of Illinois, Urbana- Champaign, IN, TR - 55, 1994.

[30] V. Gnielinski, “New equation for heat and mass transfer in turbulent pipe and channel flow,” *International Chemical Engineering*, vol. 16, pp. 359-368, 1976.

[31] M. Elliott, “Decentralized model based predictive control for a water based multi evaporator system,” M.S. thesis, Department of Mechanical Engineering, Texas A&M University, College Station, TX, 2008.

[32] L. Lennart, *System Identification, Theory for the User*, Upper Saddle River, NJ, Prentice Hall, 1999.

[33] K. Astrom and B. Wittenmark, *Adaptive Control*, Upper Saddle River, NJ, Prentice Hall, 2006.

[34] J. E. Dennis and R. B. Schabel, *Numerical Methods for Unconstrained Optimization and Nonlinear Equations*, Upper Saddle River, NJ, Prentice Hall, 1983.

[35] G. A. F Seber and C. J. Wild, *Nonlinear Regression*, New York, Wiley, 1989.

[36] K. Wang, M. Chiasson, M. Bodson, and L. Tolbert, "A nonlinear least squares approach for identification for the induction motor paramters," *IEEE Transactions on Automatic Control*, vol. 50, pp. 1622-1628, 2005.

[37] C. R. Laughman, "Fault detection methods for vapor compression air conditioners using electrical measurements," Ph.D. dissertation, Department of Electrical Engineering, Massachusetts Institute of Technology, Cambridge, MA, 2008.

[38] J. C. Langarias, J. A. Reeds, M. H. Wright, and P. E. Wright, "Convergence properties of the Nelder-Mead simplex method in low dimensions," *Society for Industrial and Applied Mathematics*, vol. 9, No.1, pp. 112-147, 1998.

[39] A. Gurson, "Simplex search behavior in nonlinear optimization," Senior thesis, Department of Computer Science, College of William and Mary, Williamsburg, VA, 1999.

[40] J. A. Nelder and R. Mead, "A simplex method for function minimization," *Computer Journal*, vol. 7, pp 308- 313, 1965.

[41] F. H. Walters, L. R. Parker, S.L. Morgan, and S. N. Deming, *Sequential Simplex Optimization*, Boca Raton, FL, CRC Press, 1991.

[42] E. Zahara and Y. T. Kao, "A hybridized approach to optimal tolerance synthesis of clutch assembly," *International Journal of Advanced Manufacturing Technology*, vol. 40, pp 1118-1124, 2009.

APPENDIX

LINEARIZED EVAPORATOR MODEL

$$\dot{\delta x} = H_x \delta x + H_u \, \delta u$$

$$\delta y = [\delta P_e; \ \delta H_{out}] = [0 \ 1 \ 0 \ 0 \ 0; 0 \ 0 \ 1 \ 0 \ 0] \ \delta x$$

$$u = \left[\dot{m}_{in} \quad \dot{m}_{out} \quad h_{in} \quad T_{a,in} \quad \dot{m}_a \right]^T$$

$$x = [L_1 \quad P_e \quad h_{out} \quad T_{w1} \quad T_{w2}]^T$$

$$\frac{\partial h}{\partial x} = H_x = \begin{bmatrix} h_{x,11} & h_{x,12} & 0 & h_{x,14} & 0 \\ h_{x,21} & h_{x,22} & h_{x,23} & 0 & h_{x,25} \\ 0 & 0 & 0 & 0 & 0 \\ h_{x,41} & h_{x,42} & 0 & h_{x,44} & h_{x,45} \\ h_{x,51} & h_{x,52} & h_{x,53} & h_{x,54} & h_{x,55} \end{bmatrix}$$

$$\frac{\partial h}{\partial u} = H_u = \begin{bmatrix} h_{u,11} & 0 & h_{u,13} & 0 & 0 \\ 0 & h_{u,22} & 0 & 0 & 0 \\ 1 & -1 & 0 & 0 & 0 \\ 0 & 0 & 0 & h_{u,44} & h_{u,45} \\ 0 & 0 & 0 & h_{u,54} & h_{u,55} \end{bmatrix}$$

Table A1 Matrix elements of the above matrices

$h_{x,11}$	$\frac{\alpha_{i1} Ai}{L_{total}} (T_{w1} - T_{r1})$
$h_{x,12}$	$-\dot{m}_{in} \left(\frac{dh_g}{dPe} \right) - \alpha_{i1} A_i \frac{L_1}{L_{total}} \frac{dT_{r1}}{dP_e}$
$h_{x,14}$	$\alpha_{i1} A_i \frac{L_1}{L_{total}}$
$h_{x,21}$	$- \frac{\alpha_{i2} A_i}{L_{total}} (T_{w2} - T_{r2})$

$h_{x,22}$	$\dot{m}_{out}\left(\frac{dh_g}{dPe}\right) - \alpha_{i2}A_i\frac{L_2}{L_{total}}\frac{\partial T_{r2}}{\partial Pe}$
$h_{x,23}$	$-\dot{m}_{out} - \alpha_{i2}A_i\frac{L_2}{L_{total}}\frac{\partial T_{r2}}{\partial h_{out}}$
$h_{x,25}$	$\alpha_{i2}A_i\frac{L_2}{L_{total}}$
$h_{x,41}$	$\alpha_o A_o\frac{\partial T_a}{\partial L_1}$
$h_{x,42}$	$\alpha_{i1}A_i\frac{dT_{r1}}{dP_e}$
$h_{x,44}$	$-\alpha_{i1}A_i - \alpha_o A_o + \alpha_o A_o\frac{\partial T_a}{\partial T_{w1}}$
$h_{x,45}$	$\alpha_o A_o\frac{\partial T_a}{\partial T_{w2}}$
$h_{x,51}$	$\alpha_o A_o\frac{\partial T_a}{\partial L_1}$
$h_{x,52}$	$\alpha_{i2}A_i\frac{\partial T_{r2}}{\partial Pe}$
$h_{x,53}$	$\alpha_{i2}A_i\frac{\partial T_{r2}}{\partial h_{out}}$
$h_{x,54}$	$\alpha_o A_o\frac{\partial T_a}{\partial T_{w1}}$
$h_{x,55}$	$-\alpha_{i2}A_i - \alpha_o A_o + \alpha_o A_o\frac{\partial T_a}{\partial T_{w2}}$
$h_{u,11}$	$h_{in} - h_g$
$h_{u,13}$	$\dot{m}_{in}$

$h_{u,22}$	$h_g - h_{out}$
$h_{u,44}$	$\alpha_o A_o \frac{\partial T_a}{\partial T_{ai}}$
$h_{u,45}$	$\frac{\partial \alpha_o}{\partial \dot{m}_{air}} A_o (T_a - T_{w1}) + \alpha_o A_o \frac{\partial T_a}{\partial \dot{m}_{air}}$
$h_{u,54}$	$\alpha_o A_o \frac{\partial T_a}{\partial T_{ai}}$
$h_{u,55}$	$\frac{\partial \alpha_o}{\partial \dot{m}_{air}} A_o (T_a - T_{w2}) + \alpha_o A_o \frac{\partial T_a}{\partial \dot{m}_{air}}$

VITA

Name:	Natarajkumar Hariharan
Address:	3123 TAMU, College Station, TX, 77843
Email Address:	nataraj.kumar@gmail.com
Education:	M.S., Mechanical Engineering, Texas A&M University, 2010 B.E., Mechanical Engineering, Birla Institute of Technology, 2007
Experience:	Graduate Research Assistant, TAMU Dept. of Mech. Engr. 08/2008-05/2010, College Station, Texas
	Graduate Teaching Assistant, TAMU Dept. of Mech. Engr. 01/2008-05/2009, College Station, Texas